Pergamon

0306-4522(94)00493-5

Neuroscience Vol. 65, No. 2, pp. 609–631, 1995
Elsevier Science Ltd

0306-4522/95 $9.50 + 0.00

DEVELOPMENT OF DIRECT GABAERGIC PROJECTIONS FROM THE ZONA INCERTA TO THE SOMATOSENSORY CORTEX OF THE RAT

M. A. L. NICOLELIS,* J. K. CHAPIN and R. C. S. LIN

Department of Physiology and Biophysics, Hahnemann University, Philadelphia, PA 19102, U.S.A.

Abstract—The postnatal development of direct thalamocortical projections from the zona incerta of the ventral thalamus to the whisker representation area of the rat primary somatosensory cortex was investigated. Cytoarchitectonic analysis based on Nissl staining, cytochrome oxidase histochemistry and immunohistochemistry for glutamic acid decarboxylase, GABA, parvalbumin and calbindin D28K revealed that the zona incerta can be clearly distinguished from surrounding diencephalic structures from the day of birth. Moreover, four distinct anatomical subdivisions of this nucleus were identified: the rostral, dorsal, ventral and caudal. Of these, the ventral subdivision is by far the most conspicuous, containing the highest density of neurons, and the highest levels of cytochrome oxidase, glutamate decarboxylase, GABA, parvalbumin and calbindin D28K. In contrast, the dorsal, rostral and caudal subdivisions contain fewer cells, lower levels of glutamic acid decarboxylase and GABA and very few parvalbumin-positive and calbindin-positive neurons. Small injections of rhodamine coated microspheres or Fluoro-gold in the primary somatosensory cortex of animals at different stages of development revealed the existence of retrogradely labeled neurons in the rostral and dorsal subdivisions of the zona incerta from postnatal day 1. At this age, retrogradely labeled cells were also found in the ventral lateral, ventral posterior medial, posterior medial, centrolateral, ventral medial and magnocellular subdivision of the medial geniculate nuclei of the dorsal thalamus. The density of the incertocortical projection reaches its maximum between the first and second postnatal weeks, decreasing subsequently, until an adult pattern of labeling is achieved. Tracer injections combined with immunohistochemistry revealed that the majority of the incertocortical projection derives from GABAergic neurons, implying a potentially inhibitory role for the incertocortical projection.

These results demonstrate that the rat trigeminal system contains parallel thalamocortical pathways of opposite polarity, emerging from both the dorsal (glutamatergic, excitatory) and ventral (GABAergic, inhibitory) thalamus since the day of birth. As such, these findings suggest that, contrary to the classical notion, not only the dorsal but also the ventral thalamus may play a special role in both cortical maturation and function.

*To whom correspondence should be addressed at: Department of Neurobiology, Box 3209, Duke University Medical Center, Durham, NC 27710, U.S.A.

Abbreviations: BSA, bovine serum albumin; C, caudal; CL, centrolateral nucleus; CO, cytochrome oxidase; CP, cerebral peduncle; d, dorsal; EML, external medullary lamina; FF, fields of Forel; FG, Fluoro-gold; GAD, glutamic acid decarboxylase; dLG dorsal lateral geniculate nucleus; H_2, fasciculus lenticularis; LH, lateral hypothalamus; LP, lateral posterior nucleus; ml, medial lemniscus; MG, medial geniculate complex; MGM, pars magnocellular of the medial geniculate nucleus; ml, medial lemniscus; MT, mamillothalamic tract; OT, optic tract; P, postnatal day; PO, posterior nucleus; POm, posterior medial nucleus; r, rostal; RCMs, rhodamine-coated microspheres; RT, reticular nucleus of the thalamus; SC, superior colliculus; SG, suprageniculate nucleus; SI, primary somatosensory cortex; SN, substantia nigra; ST, subthalamic nucleus; v, ventral; VA, ventral anterior nucleus; VL, ventral lateral nucleus; vLG, ventral lateral geniculate nucleus; VM, ventral medial nucleus; VP, ventral posterior complex; VPM, ventral posterior medial nucleus; ZI, zona incerta; ZIc, caudal subdivision of the ZI; ZId, dorsal subdivision of the ZI; ZIr, rostral subdivisions of the ZI; ZIv, ventral subdivisions of the ZI.

According to Jones,[27] the existence of distinct dorsal and ventral thalamic subregions was first suggested by Herrick's studies on the development of the amphibia diencephalon.[21] In mammals, the validity of this thalamic organization scheme was not only confirmed,[27] but further refined by the report that only neurons located in the dorsal thalamus project directly to the neocortex.[56] Over the years, thalamocortical projections were proven to be fundamental not only for the normal function of the cortex,[27,68] but also for its proper development.[16,17] Conversely, the lack of evidence for cortically projecting neurons in the ventral thalamus seemed to argue against any significant role of its nuclei in cortical maturation or function.

The ventral thalamus includes the ventral lateral geniculate nucleus (vLG), the thalamic reticular nucleus (RT) and the zona incerta (ZI). Neurons located in the vLG and the RT have not been demonstrated to project to the cortex. Until very recently, ZI neurons were also believed to project

only to subcortical structures. Nevertheless, in the last few years several independent studies have demonstrated that injections of neuroanatomical tracers in different cortical fields can produce retrograde labeling not only in the dorsal thalamus, but also in the ZI of the ventral thalamus.[14,33,37,51,57,58] Experiments conducted in our laboratory confirmed these previous observations and revealed that direct incertocortical projection in rats originate from GABAergic projection neurons.[37] Cortically projecting GABAergic neurons were found to be distributed in a rough corticotopic organization within the ZI,[37] and more incertocortical neurons were found to project to the primary somatosensory (SI) cortex than to any other cortical area. Injections of fluorescent anterograde tracers in the ZI demonstrated that incertocortical projections target mainly layer I of the SI cortex.[48] In addition, this incertocortical pathway appeared to be considerably denser in young rats.[37]

Taken together, these results point to an alternative organization of thalamocortical projections in rats in which multiple glutamatergic projections from the dorsal thalamus coexist with a parallel, potentially inhibitory, GABAergic pathway from the ventral thalamus. Given the fundamental role played by GABA in both cortical function and plasticity,[28] such a proposition considerably alters the current perception about the functional significance of the ventral thalamus. In addition, GABA in isolation, or in a balanced combination with glutamate has been shown to act as a neurothrophic factor,[4,40–42] promoting dendritic growth "*in vitro*".[40–42] Thus, GABAergic thalamocortical projections from the ventral thalamus, if present during early postnatal life, could play a special role in early stages of cortical development. This unexplored hypothesis was addressed in the present study by experiments aimed at investigating the postnatal development of incertocortical projections to the SI, and its relationship to the parallel maturation of glutamatergic thalamocortical projections from the dorsal thalamus. In these experiments, restricted injections of fluorescent retrograde tracers were placed in the SI cortex of rats at different stages of postnatal development [from postnatal day (P) 1 to adulthood] to define the distribution and density of retrograde labeling in both the dorsal and ventral thalamus. Immunohistochemistry for GABA and glutamic acid decarboxylase (GAD) was then carried out in the same tissue to identify the presence of cortically projecting GABAergic neurons in the ZI during different stages of development.

EXPERIMENTAL PROCEDURES

The postnatal development of incertofugal projections to the SI cortex was investigated by injecting retrograde fluorescent tracers, rhodamine coated microspheres (RCMs) or Fluoro-gold (FG), in 64 Long Evans (hooded) rats (Charles Rivers) ranging in age from P1 to adulthood. By convention, P1 was defined as the first 24 h after birth. Nine to twelve week old rats were considered adult animals. Sixty-four animals were studied as follows: P1, $n = 7$; P4, $n = 6$; P7, $n = 12$; P14, $n = 10$; P21, $n = 14$; P30, $n = 4$; adult, $n = 11$.

Surgery and injections

Litters of untimed pregnant rats were used for all experiments. Neonates (from P 1 to postnatal week 1) were anesthetized by hypothermia. Young (from postnatal week 2 to week 4) and adult animals received a single injection of pentobarbital (i.p. 50 mg/kg) as anesthesia. In neonates, a blade was used to make small holes in the skull overlying the presumptive positions of the SI cortex. Restricted craniotomies were performed on young and adult rats. In all cases, Hamilton syringes mounted in micromanipulators attached to the stereotaxic frame were used to manually inject small amounts of either RCMs (0.1–0.6 μl) or FG (0.1–0.3 μl) into the cortex. Tracer injections were centered in the presumptive whisker representation in the SI cortex (the "barrel fields"[77]). The total volume of RCMs or FG was distributed equally at three different depths, during a single penetration into the cortex of young and adult animals, in order to create a continuous and discrete vertical column of tracer, spanning all cortical layers. Great care was taken to produce restricted injection sites and avoid tracer spread over either the white matter or subcortical structures. Usually, larger amounts of tracer were injected in adult animals (0.6–1.0 μl). For comparative purposes, two adult rats received multiple injections of retrograde tracer (1.0 μl) distributed across the entire SI cortex.

Histology and data analysis

Two to seven days after the trace injection, animals were deeply anesthetized with pentobarbital (i.p. 50 mg/kg) and transcardially perfused with 0.9% saline followed by either 4% formalin or 3.5% paraformaldehyde in 0.1 M phosphate buffer (pH 7.4). The brains were then removed and kept overnight at 4°C in the same fixative solution, containing 20% sucrose, and then sectioned coronally or sagittally at 40–100 μm with a freezing microtome or a vibratome. Sections were mounted on gelatine-coated slides, air dried at room temperature and coverslipped before analysis. Alternate sections were counter-stained for Nissl or cytochrome oxidase (CO). Since sites of RCMs injections persisted after the CO staining process, sections stained for CO were also used to determine the precise location of cortical injection sites within the barrel fields (see results below). Only cases in which tracer injections were found to be restricted to the cortical plate of the presumptive SI were considered for further analysis. The distribution and relative density of retrogradely labeled neurons in the diencephalon were studied using an epifluorescence microscope (Nikon). Line drawings were obtained with a camera lucida attachment. The pattern of labeling in the whisker representation area of the ventral posterior (VP) complex was used to select comparable cases at different ages. For each case, high power photomicrographs were taken of the retrograde labeling observed within the ZI. For selected cases, representing particular age groups, the number of retrogradely labeled cells within the ZI was counted in every other section. The remaining sections were used for Nissl and CO staining, as described above. For each case, a total number of retrogradely labeled cells in the ZI was obtained by summing the subtotals obtained in each section analysed. Since counts were obtained in alternate, 100 μm thick sections, no correction for possible double counts was performed. Variation in the number of retrogradely labeled cells present during development was tested using a one-way analysis of variance. Testing for significant differences between individual pairs of means, representing cell counts at different postnatal ages, was carried out using a Newman–Keuls test.

Immunohistochemistry

Antibodies to the synthetic enzyme GAD (a gift from Dr D. E. Schmechel) and to GABA (Incstar Co.) were used as

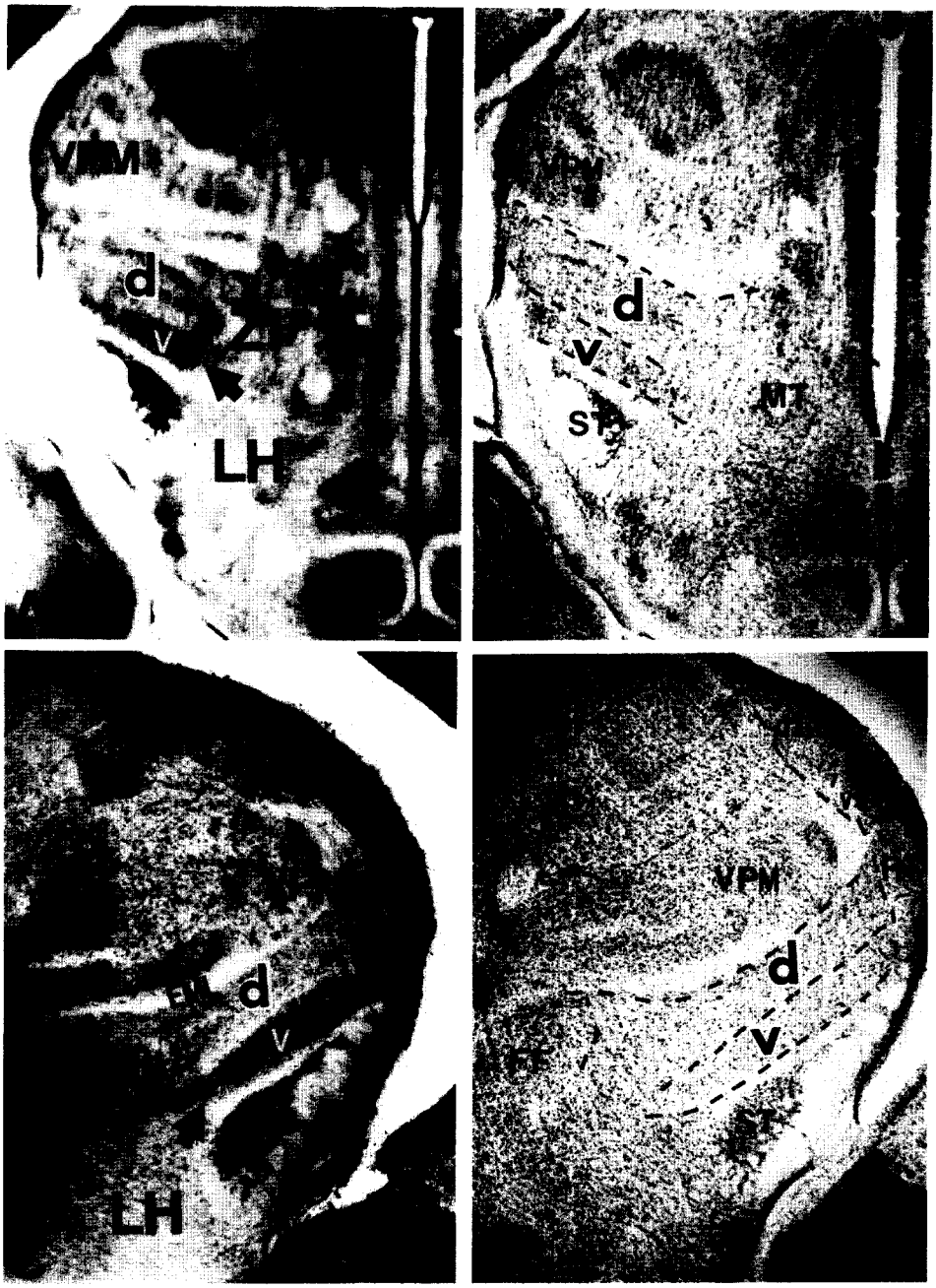

Fig. 1. Characterization of the dorsal (d) and ventral (v) subdivisions of the ZI in CO (A and C) and Nissl (B and D) stained coronal sections through the thalamus of one day old (A and B) and one week old (C and D) rats. Notice that characteristic dense CO staining of ZIv is already present on P1 (arrow head in A). At this age, the ZI occupies a substantial portion of the ventral thalamus. No clear difference in cell density can be observed between ZId and ZIv (B). At the end of the first postnatal week the intense CO staining in the ventral half of the nucleus is very clear (arrowhead in C). Dashed lines in (B) and (D) represent the dorsal and ventral boundaries of the ZI and the ZId/ZIv border. Scale bar in A (valid for all plates) = 1 mm.

specific markers for GABAergic neurons. For this procedure, 2–4 week ($n = 12$) old rats were anesthetized with sodium pentobarbital (i.p., 50 mg/kg) and then perfused through the heart with 0.9% saline, followed by 3.5% paraformaldehyde in 0.1 M phosphate buffer (pH 7.4). Brains were kept overnight in the same fixative solution and subsequently immersed in 20% sucrose in 0.1 M phosphate buffer (pH 7.4). Serial 40-μm thick coronal sections were cut with either a vibratome or a freezing microtome. Alternate sections throughout the ZI were then processed for GAD or GABA immunohistochemistry. To carry out this procedure, sections were first incubated in 0.1 M phosphate buffer (pH 7.4) containing 10% normal donkey serum for 30 min. For GAD immunohistochemistry, sections were kept overnight at 4°C in sheep anti-GAD (dilution 1:1,000–2,000 in 0.25 M Tris buffer). They were then incubated in biotinylated

donkey anti-sheep IgG (1:100 dilution with 1% normal donkey serum for 45 min–1 h). GABA immunohistochemistry was carried out by keeping sections overnight at 4°C in antiserum to GABA (rabbit anti-GABA, polyclonal) at a dilution of 1:1,000–1:2,000 in 0.1 M phosphate buffer. Subsequently, sections were incubated in biotinylated goat anti-rabbit IgG (1:100 dilution with 1% normal goat serum for 45 min–1 h. After rinsing, the sections were incubated in peroxidase–antiperoxidase complex. Every step of incubation was followed by three washes in 0.1 M phosphate buffer. The final reaction product was obtained with an intensified method, by incubating the tissue for 15–20 min in a solution of 3'3-diaminobenzidine tetrahydrochloride.[2] Sections were then mounted in gelatin-coated slides and coverslipped. Alternate sections, not reacted for GAD or GABA antibodies, were stained for Cresyl Violet or CO and

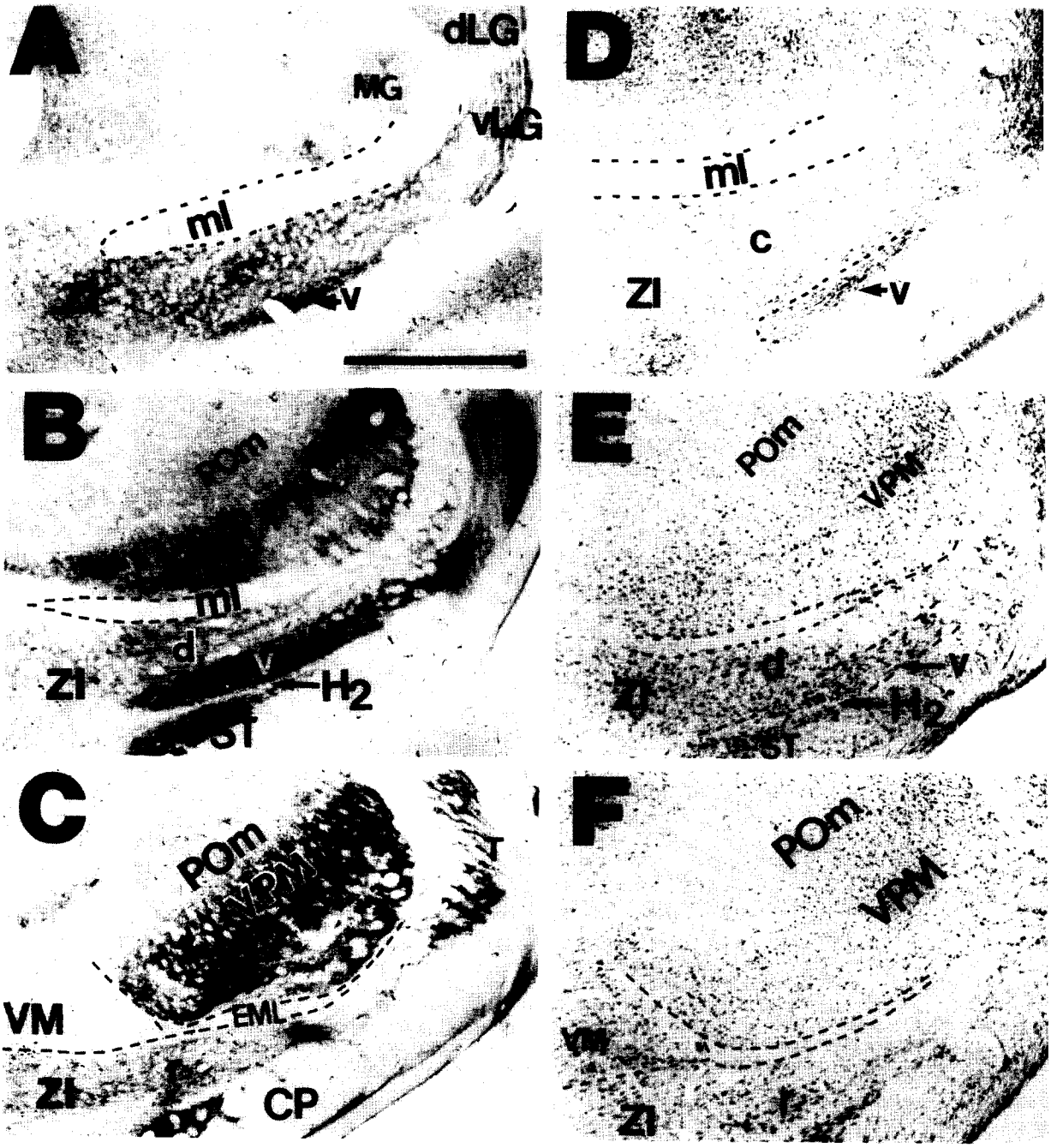

Fig. 2. Characterization of the ZI subdivision in a three week old rat. Adjacent coronal sections, at different caudal to rostral thalamic levels, stained for CO (A, B and C) and Nissl substance (D, E and F) illustrate the anatomical relationships between multiple ZI subdivisions and surrounding diencephalic structures. Notice that at this age, the ZIv exhibits a greater concentration of CO (B) and a higher cell density (E) than any other subdivision (ZIr, ZId and ZIc) of the nucleus (A, C, D, F). Dashed lines outline the area occupied by the ml and EML as well as the borders between the ZIr and the VM nucleus. Scale bar in A (valid for all plates) = 1 mm. d, dorsal and v, ventral subdivisions of the ZI.

then coverslipped. In double-labeling experiments involving RCMs and GAD or GABA immunohistochemistry, animals first received an injection of RCMs into the SI cortex. After a survival time of four days, they were perfused (as described above) and the brains were processed for GAD or GABA immunohistochemistry. Since visualization of RCMs is undiminished by the immunohistochemistry process, double-labeled cells could be directly observed in the same section under the epifluorescence microscope. Bright and epifluorescence photomicrographs of the same section were taken at different levels of illumination to document cells containing RCMs (cortical projection neurons) and/or immunoreactive to GAD or GABA antibodies.

Immunohistochemistry for parvalbumin and calbindin D28k was also carried out at different stages of development to further characterize the subdivisions of the ZI and its borders with surrounding structures. To perform these procedures, brain sections were first incubated overnight at 4°C in antiserum to parvalbumin (monoclonal antibody, dilution 1:50–500; Sigma Co, a gift from Dr M. R. Celio and Swant Co) or calbindin D28k (monoclonal antibody, dilution 1:50–500, a gift from Dr M. R. Celio and Swant Co) in a solution containing 0.1% Triton-X100, 2% BSA. Subsequently, sections were rinsed three times in 0.1 M phosphate buffer (pH 7.4) and incubated in fluorescein isothiocynate, rhodamine isothiocynate or Texas Red-conjugated anti-mouse IgG (dilution 1:50–200) at room temperature for 1 h. Sections were then rinsed and mounted on gelatin-coated slides, and coverslipped. An epifluorescence microscope (Nikon) with appropriate filters was used for data analysis.

RESULTS

Cytoarchitectonic characteristics of the zona incerta in the developing rat

The rat ZI occupies a substantial portion of the thalamus on P1 (Fig. 1 A,B). At this age, the dorsal–ventral extent of the ZI is equivalent to the dorsal–ventral dimension of the ventral posterior medial (VPM) nucleus of the dorsal thalamus (Fig. 1A,B). Over subsequent development (Fig. 1C,D; Figs 2 and 3), however, the dorsal–ventral extent of the ZI becomes progressively thinner than the VPM.

Analysis of Nissl and CO stained sections at different postnatal ages indicates that the ZI can be parcellated into multiple subdivisions. These include the most prominent cytoarchitectonic feature of the nucleus, i.e. its cell-dense, CO-rich ventral subdivision,[32,48] which is clearly observed from P1 on (Fig. 1A,B). Heretofore, several subdivision schemes for the rat ZI have been proposed in the literature.[30,56] Even though the definition of a comprehensive classification of ZI subregions is beyond the scope of the present study, a concise scheme is proposed here, based on distinct cytoarchitectonic and immunohistochemical features. In this classification, four distinct subdivisions (rostral, ventral, dorsal and caudal) of the nucleus were identified. In fact, this scheme is a variation of the very thorough classification proposed by Kawana and Watanabe.[30] In their studies, these authors subdivided the ZI into six different regions: pars rostro-polaris, pars ventralis, pars dorsalis, pars caudalis, pars magnocellularis and pars retro-polaris. In the nomenclature adopted here, the rostral (ZIr), dorsal (ZId) and ventral (ZIv) subdivisions of the ZI correspond, respectively, to the pars rostro-polaris, pars dorsalis and pars ventralis of Kawana and Watanabe.[30] On the other hand, the caudal (ZIc) subdivision of the nucleus in our scheme includes the pars caudalis, pars magnocellularis and pars retro-polaris described by those authors.

In neonatal (Fig. 1A,B) and young rats (Figs 1C,D, 2), the ZIv comprises most of the ventral half of the middle third portion of the nucleus. ZIv is separated from the subthalamic nucleus (ST) by a thin layer of tissue, the fasciculus lenticularis or Forel's field H_2 (Fig. 2B,E). Another fine, cell-sparse layer of tissue, the fibrous lamina, separates ZIv from the ZId (Figs 1, 2B,E, 3B,C,E,F). Since CO staining is always much lighter in ZId than in ZIv, these two subregions can be clearly distinguished from the day of birth. On the other hand, ZId and ZIv cannot be clearly distinguished in terms or cell density in neonatal animals (Fig. 1B), but by the end of the third postnatal week, ZIv exhibits a higher density of cells than ZId (Fig. 2E).

Fibers from the external medullary lamina (EML; Figs 1C, 2C, 3C) and the medial lemniscus (ml; Figs 2A,B,D,E, 3B) separate the ZId from the shell of the VP, at rostral and caudal levels, respectively. At all ages studied here, scattered neurons were found within the EML and medial lemniscus fibers, throughout the rostral–caudal extent of the thalamus (Figs 1, 2 and 3). These are small to medium sized fusiform cells, which resemble typical ZI neurons and do not seem to belong to the VP complex shell.

As mentioned above, two other ZI subdivisions can be readily identified in both young (Fig. 2) and adult animals (Fig. 3): the ZIr and ZIc subdivisions. The ZIr (Figs 2C,F, 3D) comprises the anterior third of the nucleus, extending from the anterior border of ZIv (see solid arrow in Fig. 3E) to the most rostral limit of the ZI. ZIr is limited dorsally by the EML, ventrally by the lateral hypothalamus (LH) and the cerebral peduncle (CP) and laterally by the reticular nucleus (RT). ZIr is also characterized by less intense CO-staining than ZIv from P1 on. ZIc (Figs 2A,D, 3A) comprises the posterior third of the nucleus, extending from the caudal border of ZIv (see open arrow in Fig. 3E) to the caudal boundary of the ZI. ZIc is bounded dorsally by the medial lemniscus, dorsolaterally by the medial geniculate (MG) complex and ventrally by the substantia nigra (SN). CO density in ZIc is higher than in ZIr but much lower than in ZIv. Both ZIr and ZIc have less cells than ZIv in adult animals.

Parasagittal sections, such as the ones displayed in Fig. 3 (panels E and F), are particularly useful to illustrate the parcellation scheme of the ZI described above. The photomicrograph of a CO-stained section in Fig. 3E depicts, in an adult rat, the position of the anterior (solid arrow) and posterior (open arrow) limits of ZIv which are used to outline the caudal

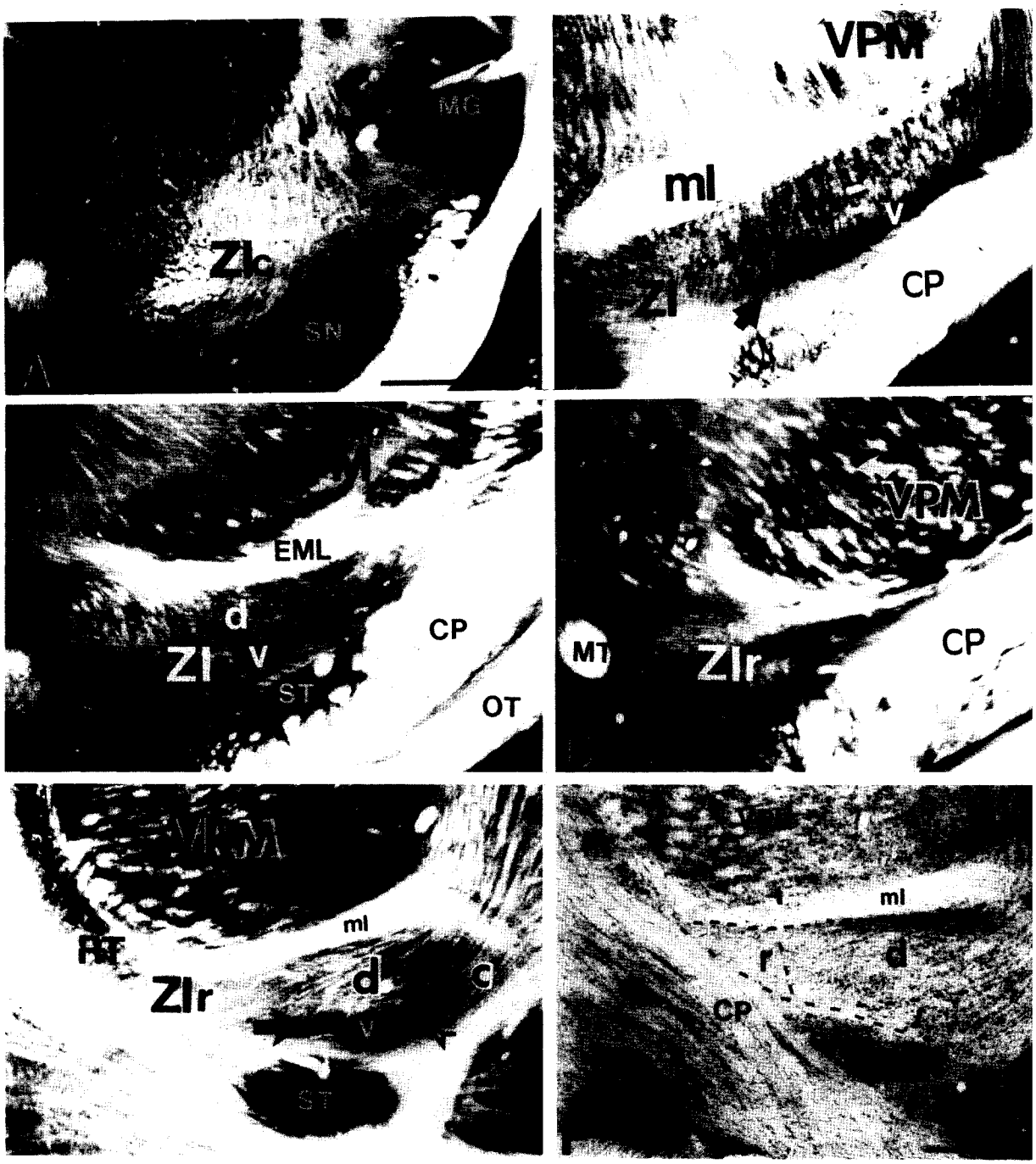

Fig. 3. The ZI and its subdivisions in the adult rat. (A–D) display the pattern of CO staining observed in coronal sections through caudal (A) to rostral (D) levels of the ZI. CO staining allowed the identification of at least four distinct subdivisions of the nucleus: the caudal (ZIc; A); dorsal (ZId; B and C), ventral (ZIv; see arrow head in B and C), and rostral (ZIr; D). This parcellation scheme can also be clearly recognized in adjacent parasagittal sections stained for CO (E) and Nissl (F). Arrows in (E) represent the anterior (solid arrow) and posterior (open arrow) limits of the CO-rich ZIv, located just dorsal to the (ST) nucleus. Scale bars in A (valid for B–D) and F (valid for E) = 1 mm.

boundary of ZIr and rostral limits of ZIc respectively. In addition, Fig. 3E illustrates the clear difference in density of CO staining across the entire rostro-caudal extension of the ZI. By comparing Fig. 3E to an adjacent Nissl stained section (Fig. 3F), it is clear that differences in CO staining density are somewhat correlated with differences in cell density. Thus, while the ZIv exhibits the highest cell density and CO staining, ZIr has the lowest density of cells and CO staining.

Immunohistochemistry for GAD, GABA parvalbumin and calbindin D28k proved very useful to characterize further the cytoarchitectonic parcellation of the ZI into multiple subdivisions, as well as to establish the borders between this nucleus and surrounding diencephalic structures. Overall, GAD and GABA immunohistochemistry yielded very similar patterns of immunoreactivity across the ZI. In fact, the distribution of GAD- and GABA-positive incertal neurons observed in young rats also matched that obtained in adult animals.[32,50] This distribution is characterized by different densities of GAD- and/or GABA-positive cells in all four subdivisions of the ZI. Typically, ZIv contains the highest concentration of GABAergic neurons in developing rats (Figs 4C, 5B,C), as well as in adult animals.[32] Nevertheless, throughout development, the distribution of GAD/GABA immunoreactive neurons within the ZI was found to be much more homogeneous than the distribution of parvalbumin, a calcium-binding protein known to be distributed in a subclass of GABAergic neurons.[8] Parvalbumin-containing neurons were

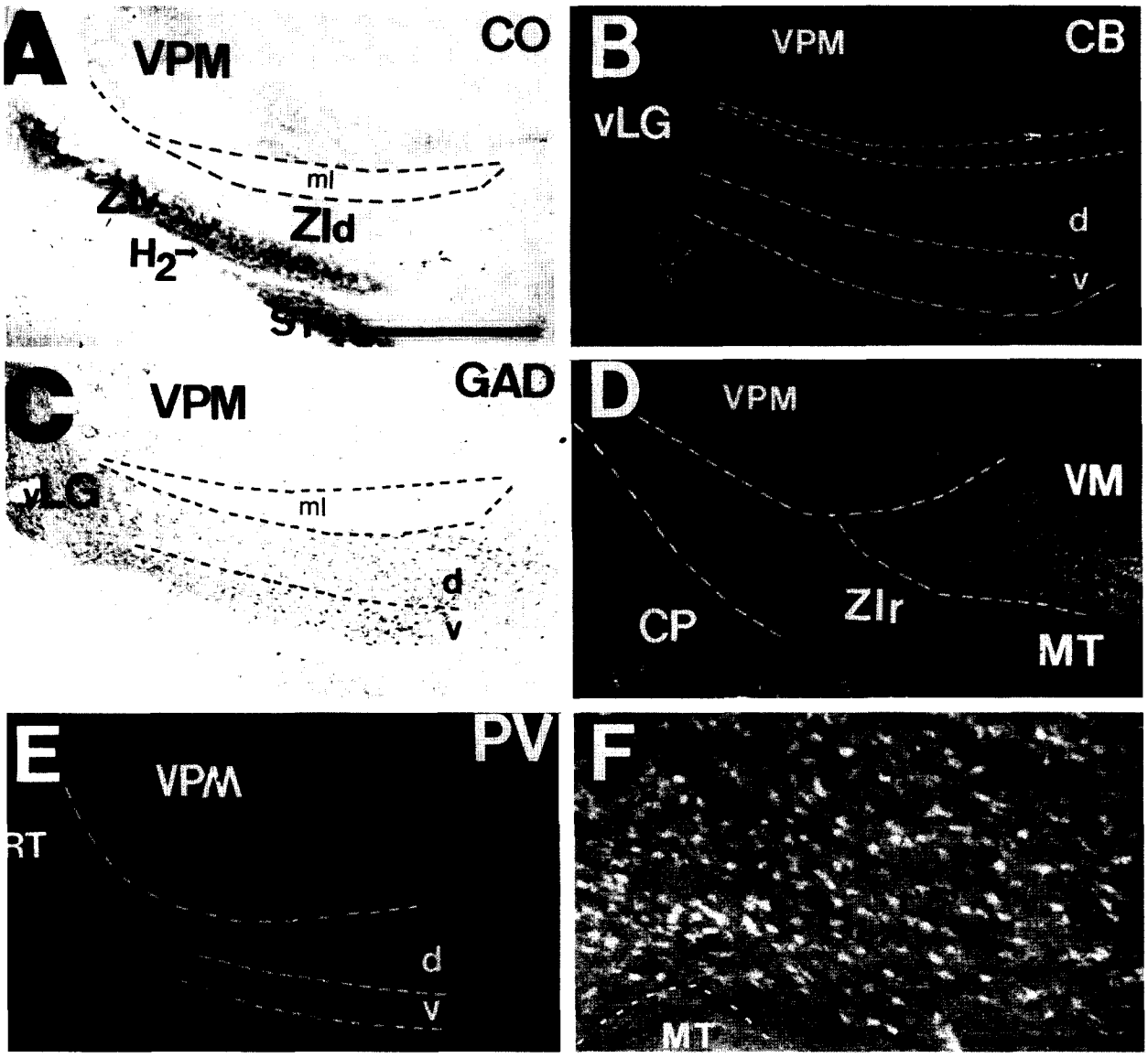

Fig. 4. Immunohistochemical characterization of distinct populations of neurons in the ZI, and borders between the ventral thalamus and the VM nucleus. Adjacent coronal brain sections, from a three week old rat, stained for (A) cytochrome oxidase (CO), (C) glutamic acid decarboxylase (GAD, ABC method) and (E) parvalbumin (PV, linked with Texas-Red) reveal the existence of distinct populations of GABAergic neurons in ZIv (high CO, GAD and PV) and ZId (Low CO, moderate GAD and very low PV). (B) ZIv neurons exhibit moderate immunoreactivity for calbindin D28k (CB, linked with Texas-Red), while only scattered neurons in ZId (B) and ZIr (D) contain this calcium-binding protein. (D and F) High immunoreactivity for calbindin (linked with Texas-Red) is observed in the VM (low power D, high power in F). Scale bar in A (valid for B–E) = 1 mm and 100 μm in F.

observed throughout the ZIv (Figs 4E, 5D), and were only sporadically found in ZIr, ZId or ZIc. Comparison of adjacent brain sections stained for CO, calbindin D28k, GAD and parvalbumin (Figs 4A,B,C,E, 5D) revealed that parvalbumin content was as good a differential marker for ZIv neurons as CO histochemistry, allowing a very precise identification of the ZIv/ZId border (Figs 4E, 5D, see dashed line). Curiously, sharper ZIv/ZId borders were observed with GAD than with GABA imunohistochemistry (compare Fig. 5B and C).

Although the ZI is a well-defined nucleus from the day of birth, some of its boundaries are sometimes difficult to identify in Nissl or CO stained sections. For instance, the boundary between the dorso-medial aspect of ZIr and the dorsomedially adjacent ventral medial nucleus (VM) may be difficult to establish in early postnatal life, since these regions tend to fuse around the lateral border of the mamillothalamic (MT) tract. These borders can be distinguished, however, by the following criteria: first, at rostral levels, VM projection neurons are mainly located dorsal and medial to the MT tract and are not immunoreactive for GAD or GABA.[60] Second, immunohistochemistry for calbindin D28k labels most VM neurons in both young and adult rats,[8,20] whereas very few calbindin D28k-positive neurons are observed in ZIr or ZId. ZIv neurons, however, are moderately labeled by calbindin D28k immunohistochemistry. This typical pattern of calbindin D28k immunoreactivity was used here to identify the ZId/ZIv border and the boundary between the ZIr and the VM nucleus (Fig. 4B,D,F).

Use of retrograde fluorescent tracers to study the postnatal development of thalamocortical projections

Very small amounts of fluorescent tracers were delivered in a single cortical penetration in each animal used in this study. Consequently, injection sites were found to be restricted to the presumptive

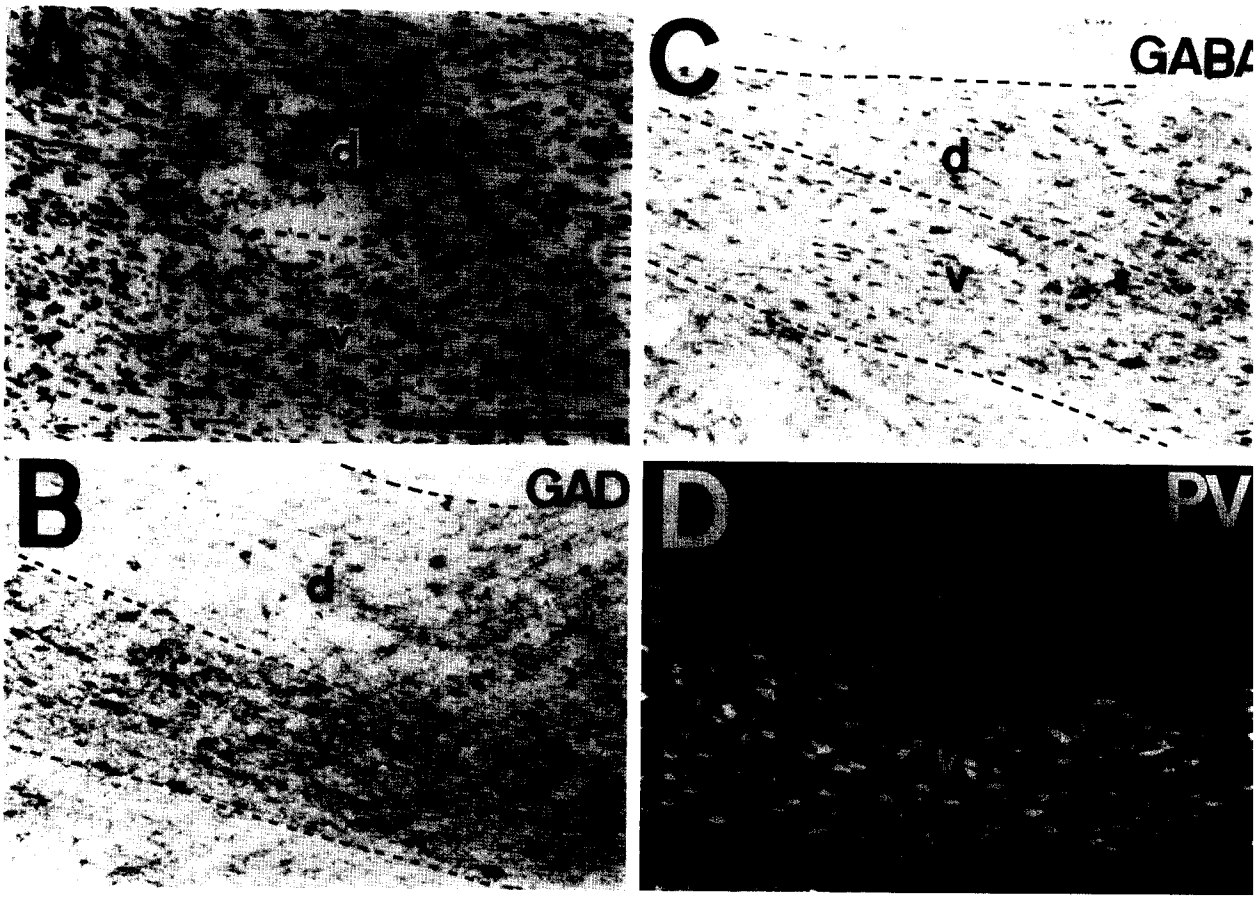

Fig. 5. Immunohistochemical characterization of the ZId/ZIv border is depicted by a series of adjacent coronal brain sections from a three week old rat. Sections were stained for Nissl substance (A), glutamic acid decarboxylase (GAD, avidin–biotin-peroxidase complex (ABC) method; B), γ-aminobutyric acid (GABA, ABC method; C) and parvalbumin (linked with Texas-Red; D). While the ZId/ZIv border can be identified in Nissl sections, it is much more reliably determined with parvalbumin since this calcium-binding protein is a specific marker for ZIv neurons. A comparison of (B) and (C) reveals that the distribution of GABA-containing neurons is relatively more homogenous across the ZI than that of GAD-positive neurons. Scale bar in A (valid for all plates) = 100 μm.

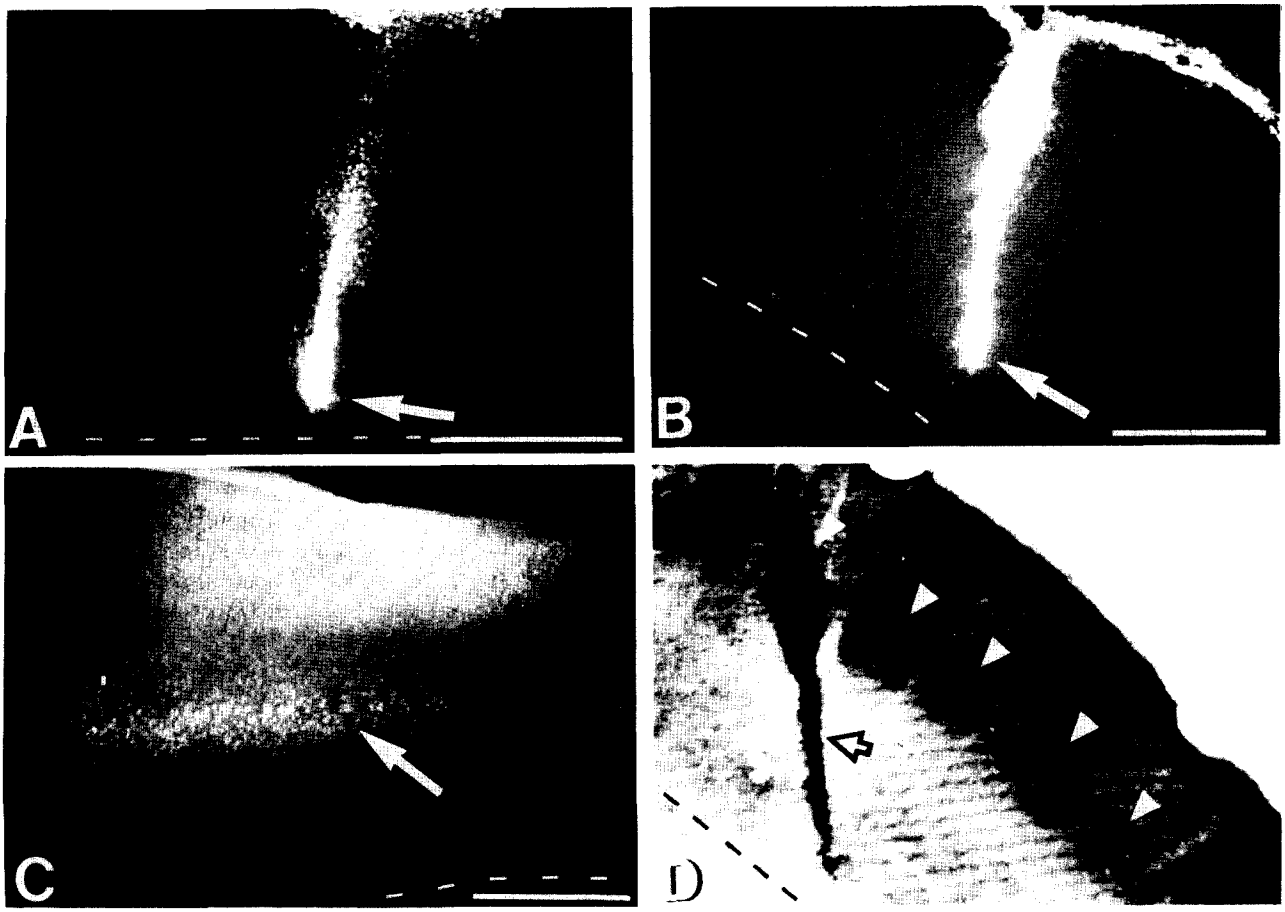

Fig. 6. Typical representation of small RCM (A, B, D) and FG (C) deposits obtained after single cortical injections of these fluorescent tracers in both young and adult rats. Very restricted column-like RCM injection sites were produced in one week (A), two week old (B) and adult (D) rats. These injections include all layers of cortex (arrows in A and B indicate ventral limit of the injection) without spreading into the underlying white matter (dorsal limit marked by dashed lines in A and B). (C) As expected, FG did not produce restricted vertical injection sites since this tracer diffuses more and produces more tissue damage than RCMs. FG injections produced extensive local labeling of corticocortical projection neurons in different layers of the cortex (solid arrow in C). (D) Detail of a column of RCMs spanning most of the cortical layers (open arrow) in the barrel fields of an adult rat after CO counterstained. The location of other barrels are indicated by arrow heads. Scale bars in A–D = 500 μm.

SI whisker area in newborn, young, and adult rats (Fig. 6). Injections of RCMs formed small vertical columns of tracer, spanning all cortical layers, without involving the underlying white matter or other subcortical structures (Fig. 6A,B). In both young and adult animals, RCMs usually did not spread more than 200–700 μm in the rostro-caudal, and mediolateral axes (including the secondary surrounding halo of tracer dispersion) of the cortex. By staining sections containing RCM injection sites for CO (Fig. 6D), we observed that the tracer spread usually involved only a few "barrels" (2–3) within the SI cortex (Fig. 6D). As expected, cortical injections of FG typically produced larger tracer spread and more tissue necrosis (Fig. 6C) than RCMs.

Even though small injection sites were produced, extensive retrograde labeling was obtained in the ipsilateral thalamus, as well as in the ipsilateral and contralateral cortices (see below). This suggests that the uptake and transport of RCMs and FG by injured cortical and thalamocortical terminals is very efficient, even when small amounts of these tracers are available in the extracellular space. Inspection of the dorsal thalamus of these animals revealed that the spatial distribution and density of retrograde labeling in the whisker representation area of the VPM nucleus was relatively similar in cases injected at different postnatal ages (Figs 7–15). This suggests that comparable injection sites were obtained in the SI cortex of animals at different stages of postnatal development, by slightly varying the amount of RCMs injected. Therefore, we relied on cases with similar injection sites and dorsal thalamic retrograde labeling distribution for our quantitative analysis (see below) of the postnatal evolution of the density of the incertocortical projection.

Postnatal development of the incertocortical projection

Injections of RCMs and FG in the SI produced retrograde labeling of ZI neurons in rats ranging in age from P1 to adulthood. In addition, these injections produced extensive labeling of both ipsi- and contralateral corticocortical projection neurons,[47] and thalamocortical projection neurons located in the dorsal thalamus. Injections on P1 (perfusion on P3) produced retrogradely labeled neurons in the following thalamic nuclei: the VPM, posterior medial (POm), centrolateral (CL), ventral anterior–ventral lateral (VA/VL), VM, magnocellular subdivision of the medial geniculate nucleus (MGM) and ZI (Figs 7 and 8). Within the dorsal thalamus, the VPM was the most densely labeled area, followed by the VM and the POm. As illustrated by the photomicrograph in Fig. 7, and the line drawing in the Fig. 8, retrogradely labeled cells in the ZI were preferentially located in the rostral two thirds of the ipsilateral nucleus, a region that spans the ZIr and ZId. No retrograde labeling was observed in ZIv and ZIc. Neurons within the contralateral ZI were rarely labeled. Little or no labeling was observed in the lateral hypothalamus at this age. On the other hand, labeled neurons were often observed within the MGM, a thalamocortical projection that is normally withdrawn at later developmental stages.[49]

The maximum density of incertocortical projections was observed during the first two postnatal weeks (Figs 9–11). Analysis of coronal sections revealed that, at this stage of development, retrogradely labeled cells within the ZI define a continuous medial to lateral strip of labeling, just ventral to the VP complex. This labeling pattern is illustrated in Fig. 9 by photomicrographs of coronal sections taken at the same diencephalic level, across the thalamus of one week old (injected on P5 and perfused on P7; Fig. 9A) and two weeks old (injected on P14 and perfused on P17, Fig. 9B) rats. Nissl stained sections (Fig. 9A′ and B′), at equivalent diencephalic levels, illustrate the main cytoarchitectonic borders identified at each stage of development.

At the end of the first postnatal week, injections of RCMs, aimed at the equivalent region of the adult "barrel fields" of the SI cortex, produced retrograde labeling within topographically appropriate regions of the VPM, POm, CL, VM, VA/VL and MGM nuclei. In addition, a dense and continuous mediolateral strip of labeling was observed in the ZI (Figs 9A,B and 10). Labeled incertal neurons formed an almost continuous antero-posterior layer within the ZI, extending from the rostral limits of the ZIr to the caudal border of the ZId (Fig. 10). Occasionally, 1–3 labeled cells were observed in the ZIc. By the end of the second postnatal week (Figs 9B and 11), labeling in the ZI was more restricted within the ZIr and ZId, a trend that would become more accentuated in the next few weeks. Retrograde labeling in the LH and in the MGM was also evident at this age.

During the third postnatal week (Fig. 12), the first signs of discontinuity were observed in the rostral to

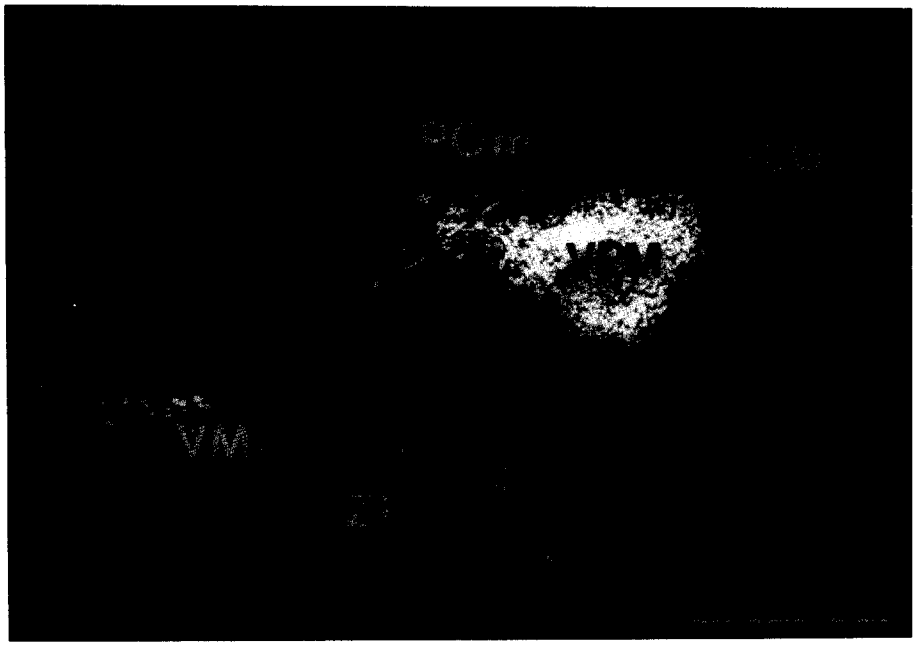

Fig. 7. Retrograde labeling of thalamic nuclei following an injection of RCMs in the SI cortex of a newborn rat injected on P1 and perfused on P3. Note intense labeling in the dorsal thalamus particularly in the VPM, POm and VM. Considerable retrograde labeling is also present in the ZI of the ventral thalamus, which at this age is already parcellated into a dorsal (d) and a ventral (v) subdivision. Scale bar = 1 mm.

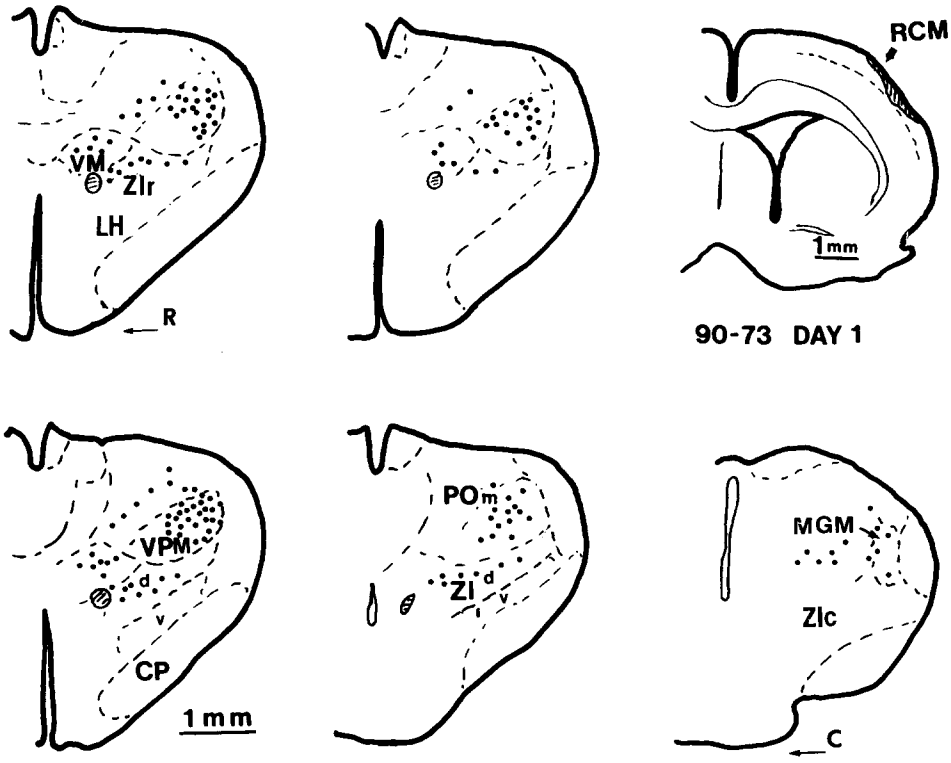

Fig. 8. Line drawing representing the distribution of retrogradely labeled neurons in the diencephalon of a newborn rat injected on P1 and perfused on P3. Retrograde labeling in the thalamus includes most of the rostrocaudal extension on the dorsal thalamus (VPM, POm, MGM and VM nuclei) and at least the most rostral two thirds of the ZI (including the ZIr and ZId, but not the ZIv).

caudal distribution of retrograde labeling in the ZI. Even though ZIr and ZId still contained most of the labeled neurons, their distribution was less compact and more restricted to the dorsal half of these subdivisions. As a result, labeling in the ZI was observed just ventral to the EML.

By the time animals reached adulthood, a thin layer of labeled cortically projecting neuron can be seen in ZIr and ZId (Figs 13, 14). This pattern is clearly depicted in the photomicrographs of Fig. 13, which contains two adjacent coronal sections through the level of the ZIr/ZId junction; one representing the distribution of retrograde labeling, and the other depicting neuroanatomical borders based upon CO histochemistry. In this case, a small injection of RCMs (Fig. 6D) in the whisker representation area of the SI cortex of an adult animal (perfused five days later) induced a very compact and restricted pattern of retrograde labeling in the VPM nucleus (small solid arrow). In addition a thin layer of labeling (borders outlined by open arrows) was observed in the ZI, extending from the lateral limit of the nucleus, where it borders the RT nucleus, all the way to the tissue surrounding the MT tract. The adjacent CO stained section clearly demonstrates that most of the labeling at the level of the ZId/ZIr border is confined to the dorsal half of these subnuclei. Serial reconstruction of sections (Fig. 14) revealed that while labeled neurons distributed along the lateral curvature of the MT belong to the ZI, those distributed dorsal to the MT tract are confined to the VM nucleus. In addition, scattered labeling in the hypothalamus, involving different nuclei in the lateral and posterior regions, is very distinct from that observed in ZIr/ZId.

Parasagittal sections through the diencephalon of animals injected at different postnatal ages (Fig. 15) were also used to investigate the pattern of thalamic labeling observed after cortical injections of RCMs. Figure 15 depicts a comparison of labeling patterns observed at the end of postnatal week 1 (Fig. 15A), week 3 (Fig. 15B), and during adulthood (Fig. 15C). Injections of RCMs produced a pattern of retrograde labeling in the thalamus resembling a crescent, which includes most of the region immediately rostral and ventral to the VP complex and the POm nucleus. The rostral head of this crescent comprises a wide area of labeling in the VA/VL and the VPM nuclei. The rostro-caudally oriented tail of the crescent begins at the level of the border between the ZI and the VP complex, and extends caudally, filling the ZIr and ZId (see Fig. 14). This tail region also contains a thin, initially continuous, but then intermittent layer of small to medium size fusiform neurons distributed across the fibers of the external medullary lamina and medial lemniscus (see solid arrow in Fig. 15B,C).

Parasagittal sections were also useful to illustrate the developmental changes imposed on the arrangement of thalamocortical projections in general, and on the distribution and density of the incertocortical system. Thus, the continuous crescent of labeling observed during the first postnatal week (Fig. 15A) gradually evolved to a more discontinuous formation (Fig. 15B), in which isolated clusters of cells belonging to the VA/VL, VPM, POm and ZI nuclei can be identified. In addition, the pattern of labeling within the ZI evolved until it reached a more restricted distribution, comprising the dorsal half of the ZIr and ZId, across the rostral two thirds of the nucleus.

Quantitative evaluation of the incertocortical projection revealed that, even though the number of retrogradely labeled neurons within the ZI remains relatively constant during the first (310 ± 39 cells, mean $\pm$ sd, $n = 3$) and second postnatal (331 ± 49, $n = 3$) weeks, a slight decline in density can be observed during the third postnatal week (242 ± 23, $n = 3$). This culminates, over subsequent development, in a three-fold reduction in the number of retrogradely labeled incertal neurons observed in adult rats (112 ± 18, $n = 3$). Multiple paired comparison using a Newman–Keuls test revealed that the difference in number of cells labeled between young (1–3 weeks old) and adult animals was statistically significant ($P < 0.01$)

To rule out the possibility that the reduced ZI labeling in adult animals was due to the creation or relatively smaller injection sites than in young animals, much larger amounts of RCMs or FG were injected in two adult animals. These involved multiple injections covering most of the SI cortex. Overall, these larger injections produced neither a higher density nor a wider distribution of retrograde labeling than observed in young animals after single cortical injections. These experiments further strengthened the evidence for an absolute reduction in the number of projecting incertocortical neurons during postnatal development.

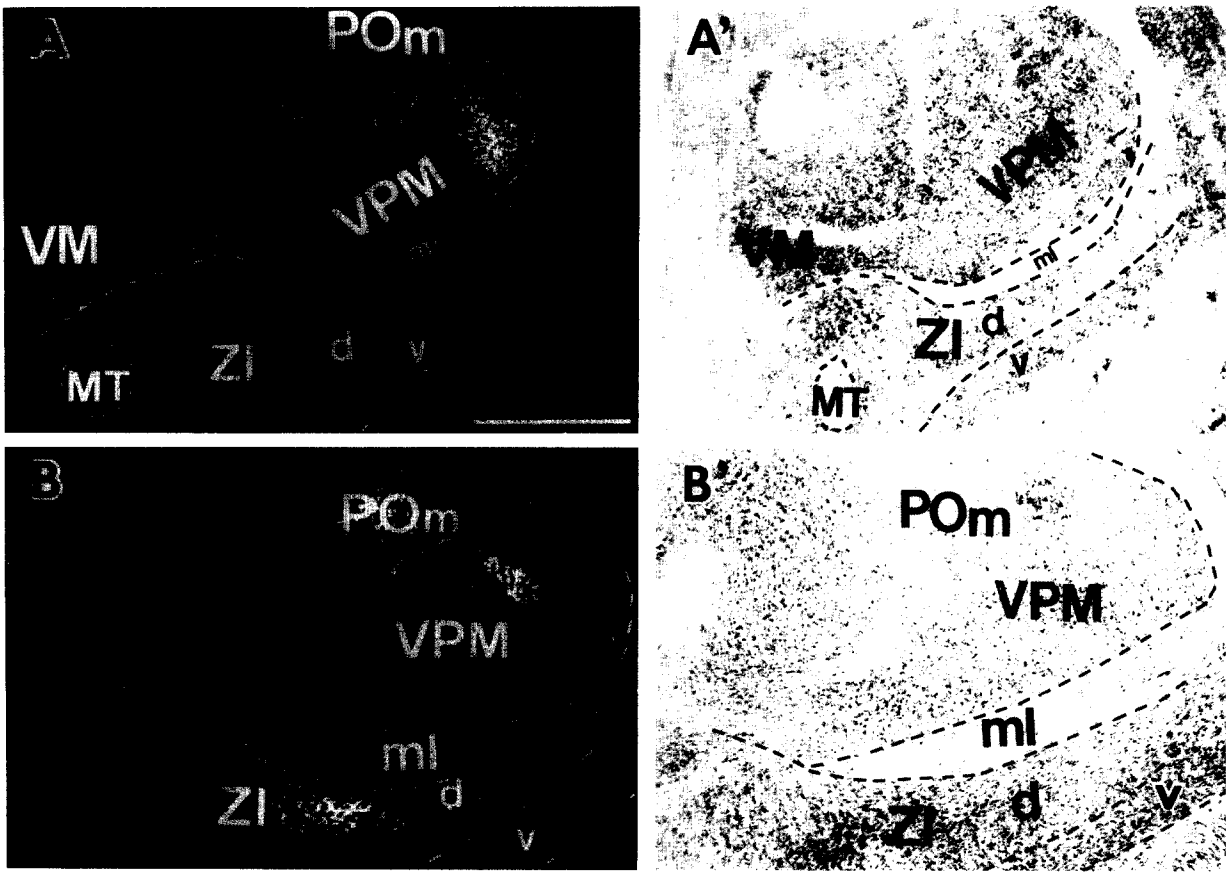

Fig. 9. Distribution of retrogradely labeled cells in the thalamus following small injections of RCMs in the SI cortex of rats at two stages of postnatal development. (A) injection on P5 perfused on P7; (B) injection on P14 perfused on P17. Dashed lines outline the boundaries of the VPM, ml and the ZId/ZIv border as depicted in Nissl stained sections (A′ and B′) at the same rostral to caudal levels. A restricted and topographic distribution of retrograde labeling within the whisker representation area of the VPM and POm at both stages of development is paralleled by massive retrograde labeling in the ZId, but not in the ZIv. Retrograde labeling is also observed in the VM nucleus. A few scattered labeled neurons are also present among the fibers of the medial lemniscus. Scale bar in A (valid for all plates) = 1 mm.

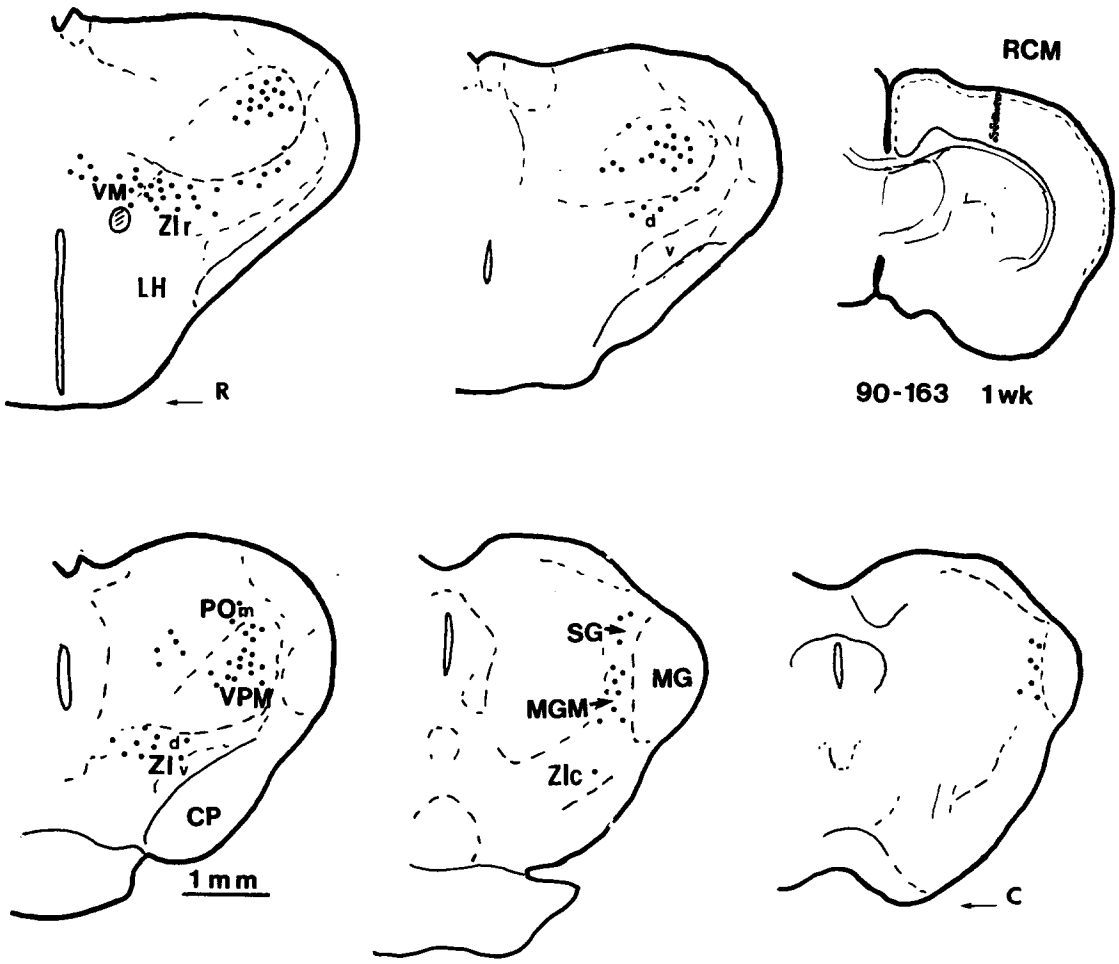

Fig. 10. Line drawing representing the distribution of retrogradely labeled neurons in the diencephalon of a one week old rat following a columnar injection of RCMs spanning most of the layers of the SI cortex. At this age labeling in the dorsal thalamus includes the POm, VPM, CL, VM and the MGM. Labeling in the ZIr and ZId is very prominent.

Immunohistochemical identity of the incertocortical pathway

Retrogradely labeled incertal neurons, which were also immunoreactive for GAD or GABA, were found ventral to the VP complex throughout the rostrocaudal extension of the ZI of young rats (2–4 weeks old). Double labeled cells were exclusively observed in ZIr and ZId of these animals. Figure 16 displays an example of double-labeled cells located in the dorsal–lateral edge of the ZId, ventral to the VP complex and dorsal to the cerebral peduncle of a three week old rat. In this figure, RCM labeled cells in the ZI (Fig. 16A,B) were also immunoreactive for GAD (Fig. 16 A′ and B′). These neurons displayed small to medium spindle shaped (coronal sections) or multipolar (sagittal sections) somata. Interestingly, cortically projecting neurons located within the fiber tracts separating the VP complex and the ZI (see description above), throughout the rostrocaudal extension of the dorsal thalamus, were occasionally labeled for GAD. A few double-labeled cells were also observed in the hypothalamus (data not shown). No GAD immunoreactivity was observed in the RCM-containing neurons within the VM, VPM, CL or POm thalamic nuclei.

DISCUSSION

Our results demonstrated that in addition to the classical projections from the dorsal thalamus, a direct ventral thalamocortical pathway is already present at birth in rats, connecting the ZI of the ventral thalamus to the whisker representation area of the SI cortex. The density of this projection is maximum during the first two postnatal weeks, declining about three-fold during subsequent development. Double-labeling studies performed in young animals (two to four weeks old) revealed that this incertocortical pathway originates mainly from GABAergic projection neurons located in the ZId and ZIr sub-divisions of the nucleus. Therefore, our results argue against the long-standing notion that

thalamocortical projections in mammals originate only from the dorsal thalamus. They further suggest a possible involvement of the ventral thalamus in both development and function of the cortex.

The hodology of the zona incerta

The identification of direct incertocortical projections enlarges the already extensive hodology of the ZI.[1,29,52,54,55,65,69,73] The main pathways targeting the ZI originate from neurons in the principal and spinal subnuclei of the trigeminal brainstem complex, the dorsal column nuclei, the SI and the motor cortices.[7,48,67] Overall, these afferents primarily target ZIv, and secondarily ZIr and ZId. The pretectum[6] is another major source of ZI input. Direct projections for the deep cerebellar nuclei[38,54] also reach the ZI. In addition, important reciprocal connections between the superior colliculus and the ZIv have been demonstrated repeatedly.[3,32]

ZI efferents are also quite diverse.[1,11,18,19,29,32,44,52,53,69,70] In a very thorough study, Ricardo[52] reported that small injections of tritiated proline and leucine placed in the ZI produced prominent anterograde labeling in several structures of the brainstem, including the middle and deep layers of the superior colliculus, pretectum and accessory oculomotor nuclei. Anterograde labeling was also observed in the spinal cord, the nonspecific thalamic nuclei, the basal ganglia and hypothalamic nuclei.

Use of more modern neuroanatomical tracers have demonstrated that cells in ZIv project primarily to the superior colliculus[32] whereas neurons in the ZIc project mainly to the brainstem and spinal cord.[48,73] More recently, the investigation of incertal projections has been complemented by the introduction of immunohistochemical methods. These studies revealed that incertal neurons can contain GABA,[32,37,48,50] dopamine,[25,37,50] somatostatin,[10] glutamate[5] and α-melanocyte-stimulating hormone (α-MSH).[33,58,66,82] GABA is by far the most prevalent neurotransmitter in the ZI, being present across all subdivisions of the nucleus in adult animals. In fact, *in situ* hybridization has shown that ZI cells contain both the α and β subunits of the rat $GABA_A$ receptor[62] and the α_1 subunit of the glycine receptor.[59] Several neuroanatomical studies combining retrograde tracers and immunohistochemistry for GAD and/or GABA have confirmed that the most prominent incertofugal projection, the incertotectal pathway, originates from GABAergic projection

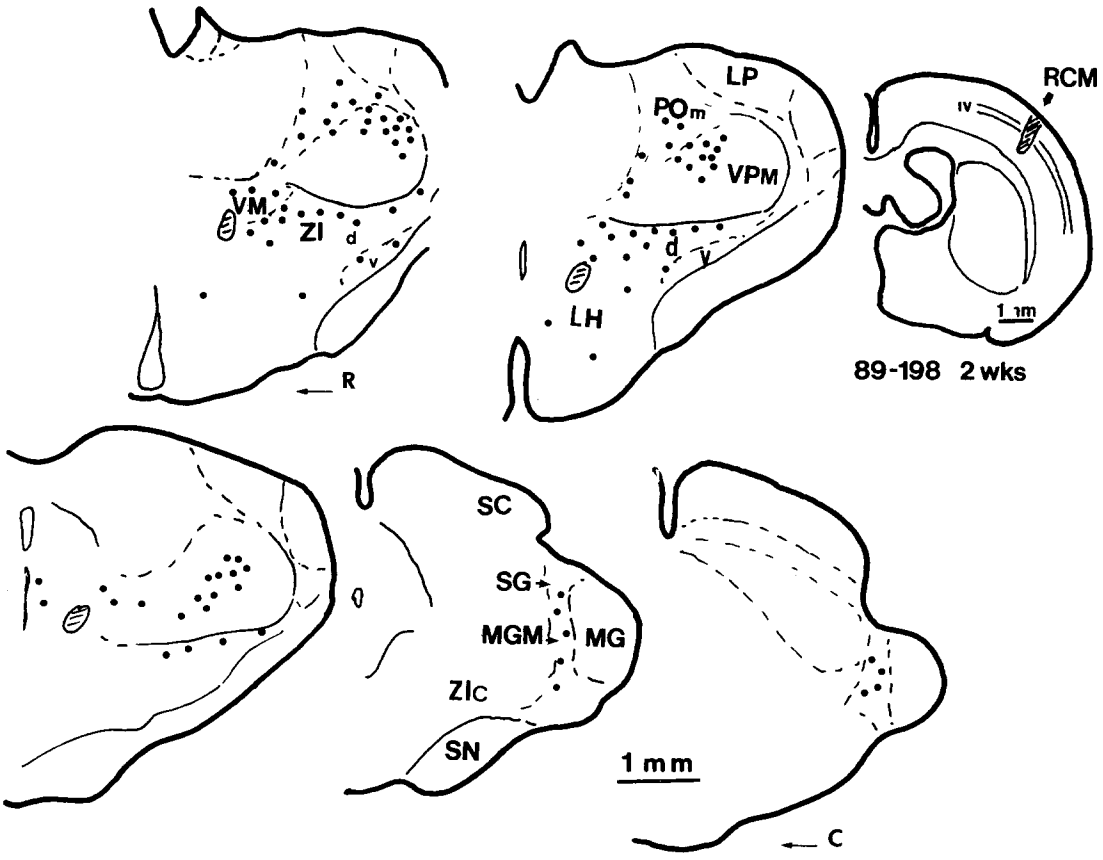

Fig. 11. Line drawing representing the distribution of retrogradely labeled neurons in the diencephalon of a two week old rat following a columnar injection of RCMs in barrel fields of the SI cortex. Labeling in the dorsal thalamus includes the POm, VPM, CL, VM and MGM. Intense and continuous labeling is also observed in the ZIr and ZId, but not in ZIv and ZIc.

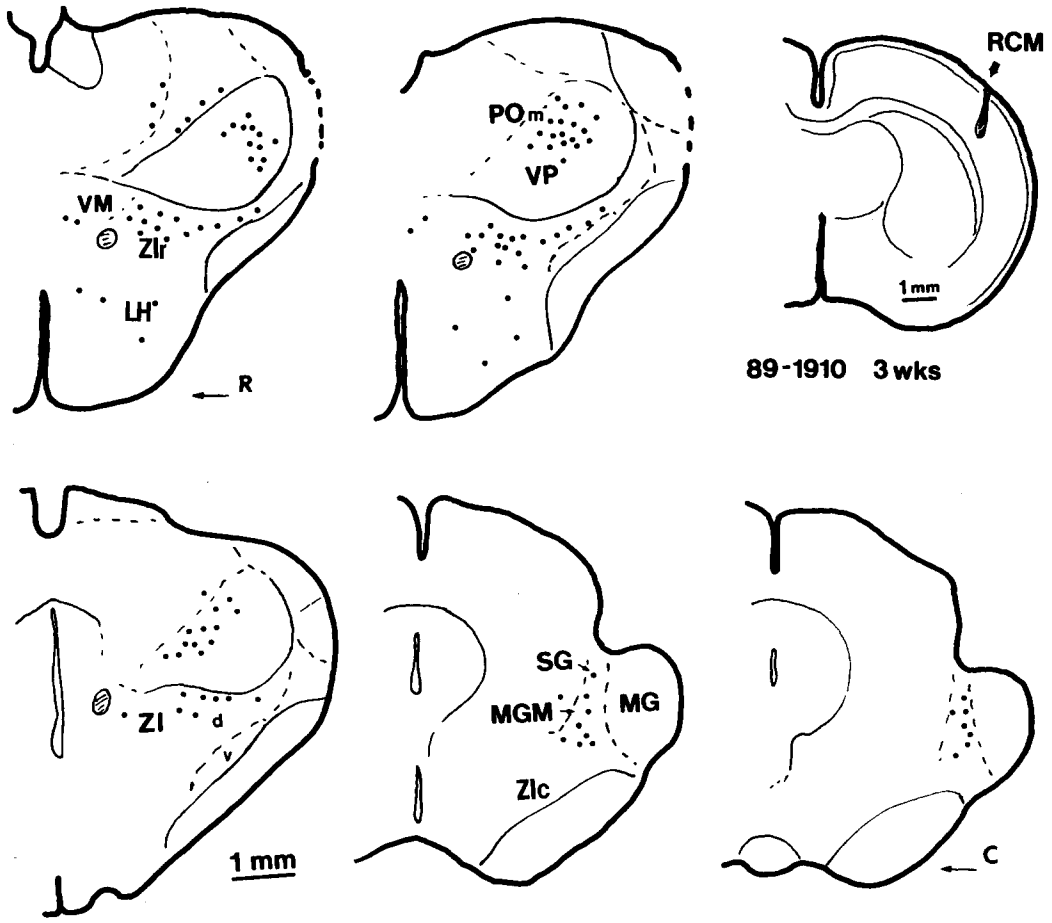

Fig. 12. Line drawing representing the distribution of retrogradely labeled neurons in the diencephalon of a three week old rat following a columnar injection of RCMs in the barrel fields of the SI cortex. At this age, the density of retrograde labeling in the ZIr and ZId begins to decline. A few labeled cells can still be seen in the MGM.

neurons.[18,32,37,38,48] Some ZI neurons also contain parvalbumin,[8,20,48] an intracellular calcium-binding protein which is present in subpopulations of GABA-ergic neurons.[8]

The incertocortical pathway

The existence of incertocortical projections in adult rats has been suggested previously by several investigators. Divac *et al.*[14] described projections from the ZI to different areas of the prefrontal cortex of rats, but provided no description of the distribution of cortically projection neurons within the subdivisions of the ZI. Shiosaka *et al.*[66] demonstrated the existence of a direct and bilateral α-MSH-containing projection from the ZI to the parietal cortex of rats. Saper[57] described the presence of retrogradely labeled cells in the rat ZI (more precisely the ZIr in our nomenclature) following injections of wheat germ agglutinin conjugated horse radish peroxidase or fluorescent dyes in different cortical areas. In another study carried out in cats, Yasui *et al.*[81] reported the existence of direct projections to the cingulate gyrus from thalamic regions lying ventral to the ventral border of the caudal two-thirds of the VP complex, a region that could span the VP shell and part of the ZI. More recently, we have reported the existence of GABA-ergic projections from the ZI to the entire neocortex[37,38] in adult rats. Since these latter reports, another neuroanatomical study has appeared confirming the existence of incertocortical projections to the frontal cortex in adult rats.[22]

Taken together, these previous observations suggest that ZI neurons project ipsilaterally to several cortical fields in rats, including sensory, limbic and association areas, with more incertal neurons projecting to the SI/MI cortices than to any other cortical area.[37] The complexity of the ZI hodology, particularly, the widespread range of its projections, has led some to postulate that the ZI is a rostral extension of the midbrain tegmentum[15,52] that could be responsible for non specific neuronal activity modulation, a physiological role commonly associated with brainstem structures such as the locus coeruleus and the raphe complex. It could be argued that the results

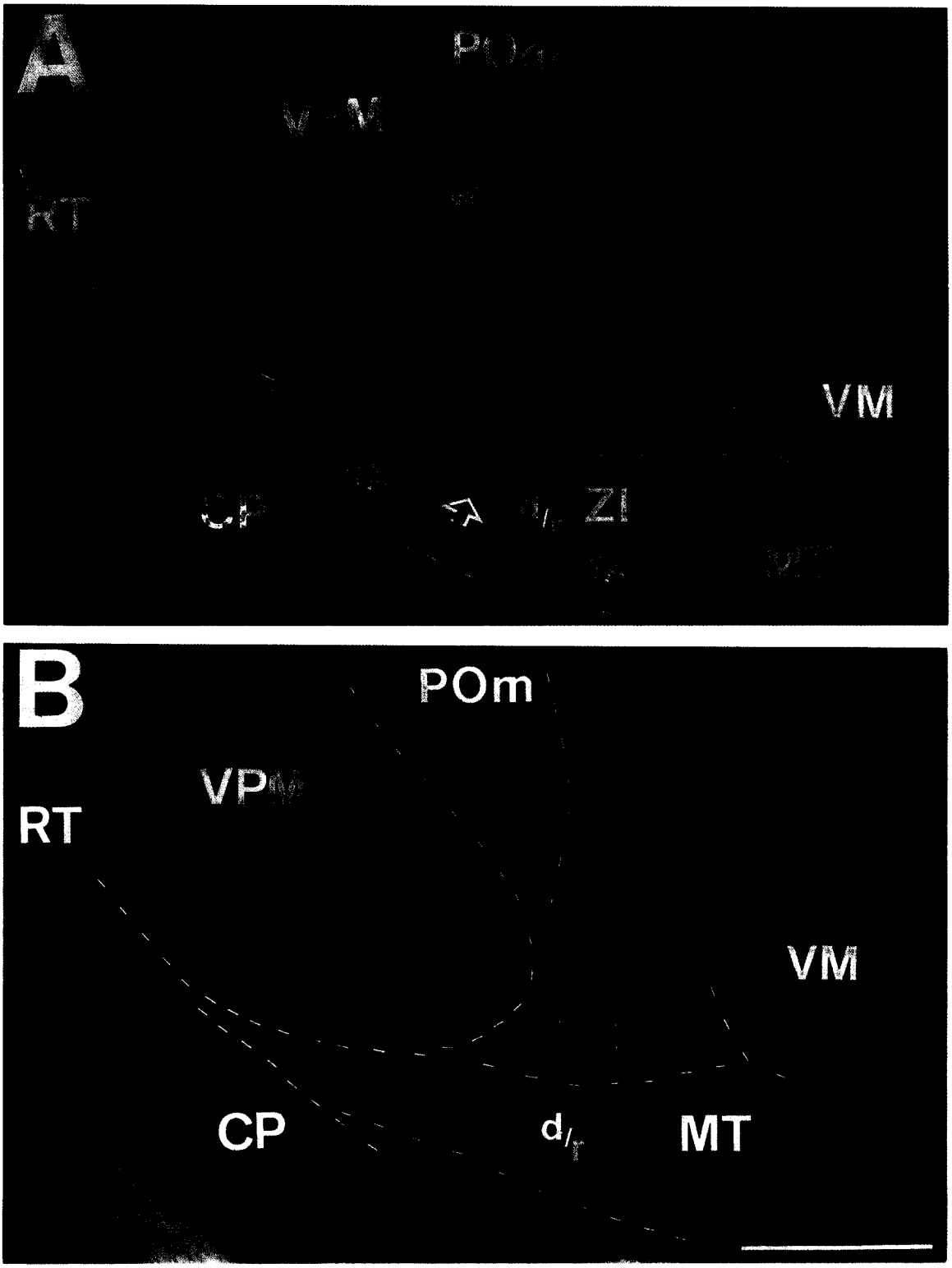

Fig. 13. Distribution or retrogradely labeled neurons in the dorsal and ventral thalamus of an adult rat following an injection of RCMs in the SI cortex. A fluorescence photomicrograph (A) of a coronal section depicts a restricted cluster of retrograde labeling in the VPM (solid arrow) and a continuous layer of labeled neurons in the ZI at the level of the ZId/ZIr border (outlined by open arrowheads). The VPM/POm (solid arrowhead), the VPM/ZI and the ZI/VM borders are drawn (dashed lines) based on an adjacent CO stained coronal section (B). Notice the clear distinction in CO staining intensity between the ZIr (latero-ventral to the MT tract) and the VM nucleus (dorso-medial to the MT tract). Scale bar in B (valid for A) = 1 mm.

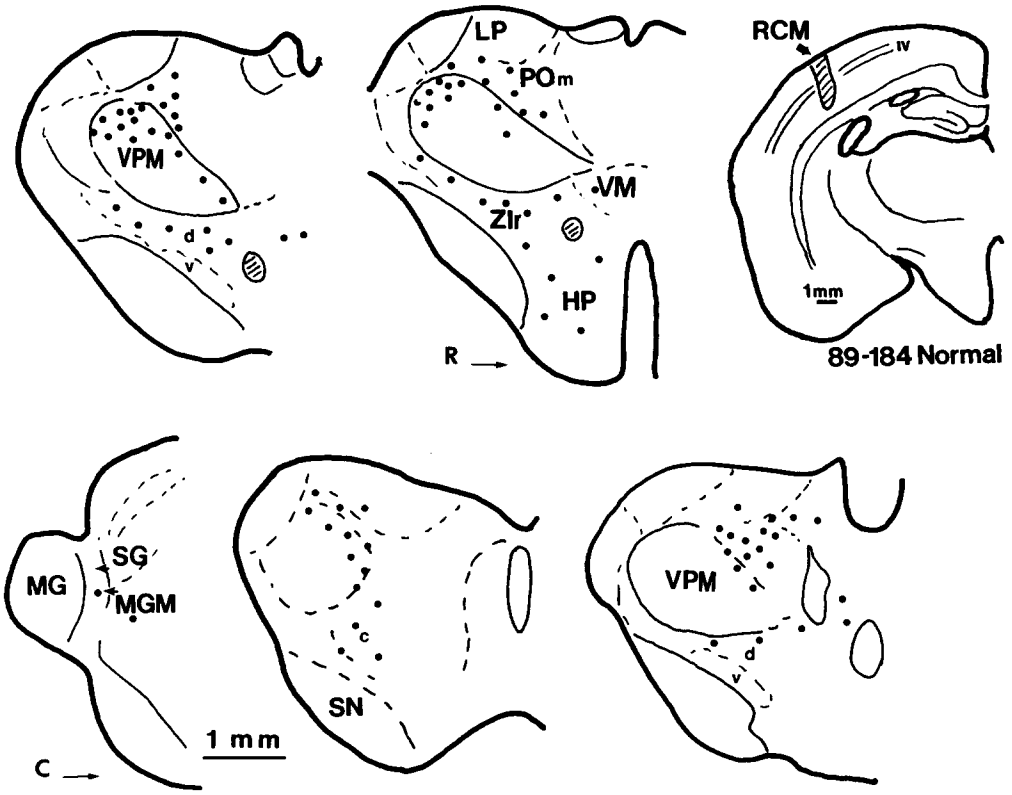

Fig. 14. Line drawing representing the distribution of retrogradely labeled neurons across different diencephalic levels of the brain of an adult rat following a columnar injection of RCMs in the barrel fields of the SI cortex. Notice that labeling in the VPM and POm nuclei remain very similar to that observed in young animals. However, labeling in the ZI is clearly reduced. In addition, only very few neurons can be identified in the vicinities of the MGM.

described here further support this hypothesis, since ascending locus coeruleus and raphe complex projections also reach the cortical mantle very early in development.[35,39,61] Moreover, both the widespread pattern of incertal projections to the neocortex, and the fact that most incertal neurons contain GABA, are reminiscent of the locus coeruleus and raphe complex projections, in that all three systems have wide access to the neocortex and a high degree of neurotransmitter specificity. Beyond this, however, no clear demonstration of a functional role for the ZI in development or neuromodulation has been presented. Despite evidence indicating that incertal neurons may be involved in the control of food and liquid ingestion[31,45,46] and sexual behaviour,[25,26] the physiological role of this conspicuous structure remains largely unknown.

The postnatal development of the zona incerta and the incertocortical system

The ventral thalamus (including the ZI, the reticular nucleus and the ventral lateral geniculate nucleus) reaches morphological maturity earlier than the dorsal thalamus during prenatal life.[43] Accordingly, heterogeneous distributions of cells and fibers, and varying degrees of CO staining are both distinct features of the ZI from the day of birth. In addition, throughout postnatal life, differences in density of GAD/GABA parvalbumin and calbindin D28k immunoreactivity indicate the existence of major ZI subdivisions, very likely containing different classes of GABAergic neurons. This argument has been reinforced by recent neuroanatomical data which demonstrated the very unique hodology of each of these subdivisions. Thus, while cortically projecting cells in ZId are immunoreactive for GAD/GABA and contain very small amounts of parvalbumin and calbindin D28k neurons belonging to ZIv contain high levels of GAD, GABA and parvalbumin, moderate immunoreactivity for calbindin D28k and project primarily to the superior colliculus.

Heretofore, no definite explanation has been proposed to account for the heterogeneity in CO staining observed across the ZI from early in postnatal life. High CO density in ZIv could simply reflect the fact that this subdivision contains a higher density of neurons and less fibers than any other ZI subregion in both young and adult animals. This hypothesis, however, does not explain why a distinct difference in CO density between ZIv and ZId is already conspicuous during the first postnatal week, even though no major difference in cell density is apparent between

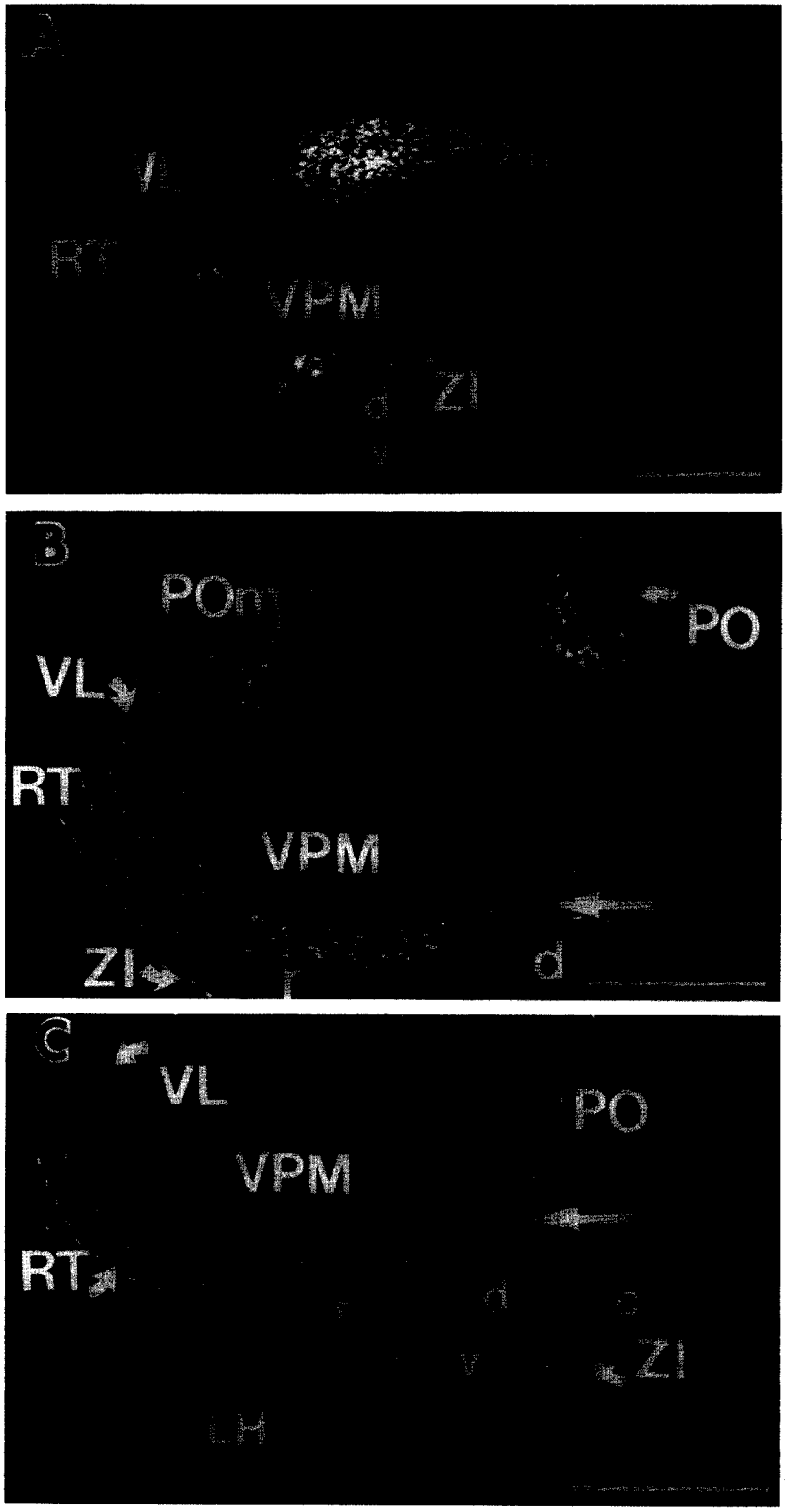

Fig. 15. Distribution of retrogradely labeled neurons as seen in parasagittal sections of the diencephalon of rats which received a single cortical injection of RCMs at different postnatal ages. (A) one week; (B) 3 weeks; (C) and adult rats. Notice that the rostral to caudal distribution of labeled neurons in the diencephalon of these animals resembles a crescent. Labeled neurons in the most rostral regions are located in the VA/VL complex. Labeled cells within the ventral and caudal regions of this ellipsoid (solid arrow in B and C) spread into the ZI and into the fibers of the external medullary lamina which separate the dorsal thalamus and the ZI. The ventral limit of the VP complex in each photomicrograph is outlined by dashed lines. Scale bars = 1 mm.

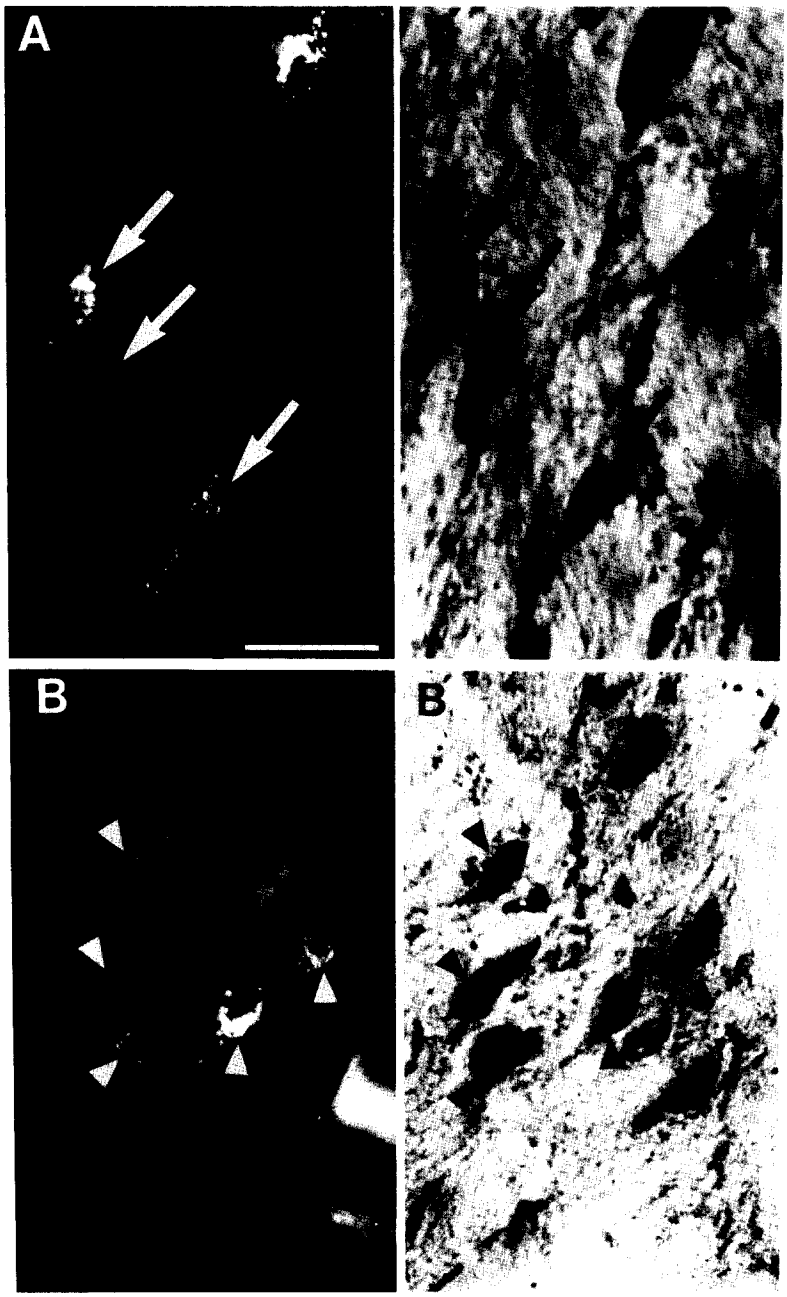

Fig. 16. Double-labeling experiments demonstrate that GABAergic incertal neurons project to the SI cortex of young rats. These matching fluorescence and brightfield photomicrographs show that retrogradely labeled incertal neurons [white arrows in (A) and arrowheads in (B)] in the ZId of a 3 week old rat, following a single injection of RCMs in the SI cortex, are also immunoreactive for GAD (black arrows in (A') and arrowheads in (B')). Scale bar in A (valid for all plates) = 25 μm.

these subdivisions at this developmental stage. Alternatively, high levels of CO could indicate high levels of neuronal activity.[75,76] In this context, projecting neurons within ZIv could exhibit much higher levels of tonic activity than other incertal neurons since early in postnatal life. Developmentally, this could also indicate that ZIv neurons reach functional maturity (e.g. adult-like levels of tonic activity) very early in postnatal life. Interestingly, an early functional maturation of the ZI has also been suggested independently by Yamamoto *et al.*[80] These authors observed a distinct immunoreactivity for connexin43, a gap junction protein found in astrocytes and cells lining brain surfaces,[78,79] in the rat ZI at early postnatal life. Yamamoto *et al.*[80] observed that a group of connexin43 profiles, defined by the predominance of immunoreactive puncta, constitutes the typical adult pattern, which begins to be established in other

structures around P15, and may reflect the time at which cells reach functional electrical maturity. In the ZI, a moderate density of puncta was observed as early as P1.[80] The early maturation of the ZI, as well as the rest of the ventral thalamus, may be required for the expression of important behaviors in newborn rats. Nevertheless, this possibility remains to be further explored.

On P1, trigeminal afferents conveying information from facial whiskers have already reached the ventral posterior complex of the dorsal thalamus and the ZI[64] (Dr S. Senft, personal communication). Our results demonstrated that at this age, projections from dorsal thalamic structures such as VPM, POm, CL and VM, but also from ZI have already reached the ipsilateral SI cortex. These results confirm previous data obtained by Senft and Woosley[63] with the anterograde transport of HRP in brain slices. These authors reported that thalamocortical afferents to the mouse SI could be identified on the day of birth. More recently, thalamocortical projections from the VP complex have been observed within the cortical plate of the barrel fields in prenatal rats using the anterograde transport of DiI.[16,17,64] Injections of the same tracer in the SI cortex in neonatal animals have also revealed the presence of retrogradely labeled neurons in the VP complex, POm and the ZI (M. Diamond, personal communication). Thus, use of modern retrograde/anterograde fluorescent tracers has demonstrated that thalamocortical projections reach the cortical plate of the rodent SI cortext at least three to four days earlier than previously reported.[74] Differences in tracer properties could also explain why projections from ZI to the SI have not been previously described in developing animals.

Altogether, these observations indicate that the rat trigeminal system is formed by parallel thalamocortical pathways, of opposite polarities, derived from the dorsal (glutamatergic, excitatory) and ventral thalamus (GABAergic, inhibitory). In fact, additional evidence supports the inclusion of some of the ZI subregions as genuine thalamic relays of the rat trigeminal system. First, the ZI also receives corticothalamic afferents originating from the MI and SI cortices,[65] as do the other dorsal thalamic relays of the ascending trigeminal system.[9] Second, we and others have demonstrated somatosensory responses in the ZI derived from the stimulation of low threshold peripheral cutaneous receptors or SI cortex.[13,34,48] The physiological role of these somatosensory responses within the ZI, however, remains unknown.

In our hands, injections of RCMs produced very intense and restricted retrograde labeling in the dorsomedial aspect of the VPM at all age groups analyzed. This stereotyped labeling pattern was used as a way to control both injection topography and injection size. However, while the density and distribution of retrogradely labeled VPM neurons did not change over subsequent postnatal development, a reasonable variation was observed in the number of labeled cells and distribution of labeling within the ZI. Thus, while the density of retrograde labeling observed in the VPM and ZI was similar in young animals, in adult animals much more labeling was observed in the VPM than in the ZI. From postnatal week 3 to adulthood, a reduction in density of incertocortical neurons was accompanied by a restriction in the distribution of those neurons within the ZI. As a result, incertocortical neurons are restricted to the dorsal half of the ZIr and ZId in adult rats.

Interestingly, a similar reduction in density of thalamocortical projections over development was observed by us in the MGM.[49] Moreover, Villalobos *et al.*[71] have recently reported a clear reduction in density of subcortical afferents to the medial frontal cortex in aged mice when compared to young animals. This reduction included a three-fold decrease in the number of incertocortical neurons. Although no experiments were performed in the latter and in the present study to clarify the mechanism involved in this process, both cell death and collateral withdrawal[12] have been suggested as possible developmental mechanisms that may account for the decrease in density of projections. Evidently, since no quantitative analysis of cell density or nucleus volume has been carried out in either study, one needs to be cautious when interpreting the reductions in labeling density observed over postnatal development.

Functional relevance of incertocortical projections

The functional relevance of the incertocortical system is directly related to the fact that this projection is mainly GABAergic and reaches the cortical plate of the rat SI very early in development. So far, the sources of GABAergic fibers observed in the neocortex during prenatal and early postnatal development have not been identified. Intrinsic cortical neurons are probably only one of the contributors to the plexus of GABAergic fibers coursing through layer I. It is also likely that some of these GABAergic fibers derive from the incertocortical neurons described here. In fact, the ZI has been shown to give rise to GABAergic projections to the midbrain very early in prenatal life.[36] Moreover, we have recently demonstrated that, in adult rats, incertal neurons project to superficial layers of the SI cortex, particularly layer I.[48] Structures such as the hypothalamus,[72] septum and different brainstem nuclei could provide most of the remaining GABAergic fibers to the neocortex.

Though the role of GABA during early development is unknown, it has been suggested that it could act as a neurotrophic factor.[4,36,41,42] Thus, GABA has been reported to influence *in vitro* neurite outgrowth[40–42] through an interesting mechanism. When GABA and its potentiator, diazepam, were added to cultured embryonic hippocampal pyramidal neurons, the subsequent growth of axons and dendrites of those cells was inhibited.[40] The same cell behavior was

observed when glutamate was used.[40] In another series of experiments, GABA–diazepam was added to a medium containing a concentration of glutamate that normally would cause dendritic regression. This combination allowed dendritic growth to advance. Mattson[41] suggested that an ideal degree of electrical activity is necessary to allow neurite outgrowth. According to this theory, an excess of either glutamate or GABA would disrupt neurite growth. However, a balanced combination of both would maintain the development of dendrites and axons.

A possible competition between GABA and glutamate, so far only demonstrated in "*in vitro*" preparations, could occur during the development of the cortex, since GABAergic fibers are in close contact with maturing glutamate-containing terminals derived from thalamocortical and corticocortical projections. GABA release could then balance potentially harmful effects of glutamate, or even interact with it in order to establish the normal cortical architecture. As such, it is interesting to note that GABAergic neurons from the ZI reach their maximal density of projection to the SI during the first two weeks after birth, a critical period for the establishment of the fine architecture of ipsilateral corticocortical, callosal and thalamocortical projections.[16,17,23,24,47]

CONCLUSIONS

The results described above demonstrate that GABAergic neurons located within the dorsal subdivision of the zona incerta constitute the main source of thalamocortical projections from the ventral thalamus to the rat primary somatosensory cortex from the day of birth. These incertocortical projections parallel the classical thalamocortical projections from multiple dorsal thalamic nuclei, suggesting that both the ventral and dorsal thalamus may play significant roles in the development and normal function of cortical networks.

Acknowledgements—We would like to thank Dr Laura M. O. Oliveira for her excellent technical assistance. This work was supported by a fellowship award from the Sao Paulo State Foundation for Research, FAPESP 88/4044-9 to Miguel A. L. Nicolelis and grants NS 26722, AAO 6965, AFOSR 90-0266 to John K. Chapin and NS 29161 to Rick C. S. Lin.

REFERENCES

1. Aas J. E. (1989) Subcortical projections to the pontine nuclei in the cat. *J. comp. Neurol.* **282,** 331–354.
2. Adams J. C. (1981) Heavy metal intensification of DAB-based HRP reaction product. *J. Histochem. Cytochem.* **29,** 775.
3. Appell P. P. and Behan M. (1990) Sources of subcortical GABAergic projections to the superior colliculus in the cat. *J. comp. Neurol.* **302,** 143–158.
4. Behar T. N., Schaffner A. E., Colton C. A., Somogyi R., Olah Z., Lehel C. and Barker J. L. (1994) GABA-induce chemokinesis and NGF-induced chemotaxis of embryonic spinal cord neurons. *J. Neurosci.* **14,** 29–38.
5. Beitz A. J. (1989) Possible origin of glutamatergic projections to the midbrain periaqueductal gray and deep layer of the superior colliculus of the rat. *Brain Res. Bull.* **23,** 25–35.
6. Berman N. (1977) Connections of the pretectum in the cat. *J. comp. Neurol.* **174,** 227–254.
7. Berkley K. J., Budell R. J., Blomqvist A. and Mark B. (1986) Output systems of the dorsal column nuclei in the cat. *Brain Res. Rev.* **11,** 199–225.
8. Celio M. R. (1990) Calbindin D-28k and parvalbumin in the rat nervous system. *Neuroscience* **35,** 375–475.
9. Chmielowska J., Carvel G. E. and Simons D. J. (1989) Spatial organization of thalamocortical and corticothalamic projection systems in the rat Sml barrel cortex. *J. comp. Neurol.* **285,** 325–338.
10. Cotter J. R. and Laemle L. K. (1987) Distribution of somatostatin like immunoreactivity in the brain of the little brown bat (*Myotis lucifugus*). *Am. J. Anat.* **180,** 280–294.
11. Covey E., Hall W. C. and Kobler J. B. (1987) Subcortical connections of the superior colliculus in the Mustache Bat, Pteronotus parnellii. *J. comp. Neurol.* **263,** 179–197.
12. Cowan W. M., Fawcett J. W., O'Leary D. D. M. and Stanfield B. B. (1984) Regressive events in neurogenesis. *Science* **225,** 1258–1265.
13. Darian-Smith I. (1964) Cortical projections of thalamic neurones excited by mechanical stimulation of the face of the cat. *J. Physiol, Lond.* **171,** 339–360.
14. Divac I., Kosmel A., Björklun A. and Lindvall O. (1978) Subcortical projections to the prefrontal cortex in the rat as revealed by the horseradish peroxidase technique. *Neuroscience* **3,** 785–796.
15. Domesick V. B. (1969) Projections from the cingulate cortex in the rat. *Brain Res.* **12,** 296–320.
16. Erzurumlu R. S. and Jhaveri S. (1990a) Thalamic afferent segregation precedes barrel formation in the rat Sl. *Proc. Soc. Neurosci.* **16,** 1214 (Abst.).
17. Erzurumlu R. S. and Jhaveri S. (1990b) Thalamic axons confer a blueprint of the sensory periphery onto the developing rat somatosensory cortex. *Devl Brain Res.* **56,** 229–234.
18. Ficalora A. S. and Mize R. R. (1989) The neurons of the substantia nigra and zona incerta which project to the cat superior colliculus are GABA immunoreactive: a double-label study using GABA immunocytochemistry and lectin retrograde transport. *Neuroscience* **29,** 567–581.
19. Foster G. A., Sizer A. R., Rees H. and Roberts M. H. T. (1989) Afferent projections to the rostral anterior pretectal nucleus of the rat: a possible role in the processing of noxius stimuli. *J. comp. Neurol.* **29,** 685–694.
20. Frassoni C., Bentivoglio M., Spreafico R., Sanchez M. P., Puelles L. and Fairen A. (1991) Postnatal development of calbindin and parvalbumin immunoreactivity in the thalamus of the rat. *Devl Brain Res.* **58,** 243–249.
21. Herrick C. J. (1910) The morphology of the forebrain in Amphibia and Reptilia. *J. comp. Neurol.* **20,** 413–547.
22. Hicks R. R. and Huerta M. F. (1991) Differential thalamic connectivity of rostral and caudal parts of cortical area Fr2 in rats. *Brain Res.* **568 (1),** 325–329.

23. Ivy G. O. and Killackey H. P. (1981) The ontogeny of the distribution of callosal projection neurons in the rat parietal cortex. *J. comp. Neurol.* **195,** 367–389.
24. Ivy G. O. and Killackey H. P. (1982) Ontogenetic changes in the projections of neocortical neurons. *J. Neurosci.* **2,** 735–743.
25. James M. D., MacKenzie F. J., Tuohy-Jones P. A. and Wilson C. A. (1987) Dopaminergic neurons in the zona incerta exert a stimulatory control on gonadotrophin release via D1 dopamine receptors. *Neuroendocrinology* **45,** 348–355.
26. James M. D., Hole D. R. and Wilson C. A. (1989) Differential involvement of 5-hydroxytryptamine (5HT) in specific hypothalamic areas in the mediation of steroid-induced changes in gonadotrophin release and sexual behaviour in female rats. *Neuroendocrinology* **49,** 561–569.
27. Jones E. G. (1985) *The Thalamus.* Plenum, New York.
28. Jones E. G. (1993) GABAergic neurons and their role in cortical plasticity in primates. *Cereb. Cortex* **3,** 361–372.
29. Kaelber W. W. and Smith T. B. (1979) Projections of the zona incerta in the cat, with stimulation controls. *Expl Neurol.* **63,** 177–200.
30. Kawana E. and Watanabe K. (1981) Cytoarchitectonic study of zona incerta in the rat. *J. Hirnforsch.* **22,** 535–541.
31. Kendrik K. M. and Baldwin B. A. (1986) Characterization of neuronal responses in the zona incerta of the subthalamic region of the sheep during ingestion of food and liquid. *Neurosci. Lett.* **63,** 237–242.
32. Kim U., Gregory E. and Hall W. C. (1992) Connections between a ventral, GABAergic subdivision of zona incerta and the superior colliculus. *J. comp. Neurol.* **321,** 555–575.
33. Kohler C., Haglund L. and Swanson L. W. (1984) A diffuse α-MSH-immunoreactive projection to the hippocampus and spinal cord from individual neurons in the lateral hypothalamic area and zona incerta. *J. comp. Neurol.* **223,** 501–514.
34. Kruger L. and Albe-Fessard D. (1960) Distribution of responses to somatic afferent stimuli in the diencephalon of the cat under chloralose anesthesia. *Expl Neurol.* **2,** 442–467.
35. Lauder J. M., Wallace J. A., Krebs H., Petruz P. and McCarthy K. (1982) *In vivo* and *in vitro* development of serotonergic neurons. *Brain Res. Bull.* **9,** 605–625.
36. Lauder J. M., Han V. K. M., Henderson P., Verdoorn T. and Towle A. C. (1986) Prenatal ontogeny of the GABAergic system in the rat brain: an immunocytochemical study. *Neuroscience* **19,** 465–493.
37. Lin C. S., Nicolelis M. A. L., Schneider J. S. and Chapin J. K. (1990) A major direct GABAergic pathway from zona incerta to necocortex. *Science* **248,** 1553–1556.
38. Lin R. C. S., Nicolelis M. A. L., McLean J. and Chapin J. K. (1991) The topographic organization of the rat zona incerta. *Proc. Soc. Neurosci.* **17,** 290.
39. Marin-Padilla M. (1984) Neurons of layer I. A developmental analysis. In *Cerebral Cortex* (eds Peters A. and Jones E. G.), Vol. 1, pp. 447–478, Plenum, New York.
40. Mattson M. P., Dou P. and Kater S. B. (1987) Pruning of hippocampal pyramidal neuron dendritic architecture in vitro by glutamate and a protective effect of GABA plus diazepam. *Proc. Soc. Neurosci.* **13,** 367.
41. Mattson M. P. (1988) Neurotransmitters in the regulation of neuronal cytoarchitecture. *Brain Res. Rev.* **13,** 179–212.
42. Mattson M. P. and Kater S. B. (1989) Excitatory and inhibitory neurotransmitters in the generation and degeneration of hippocampal neuroarchitecture. *Brain Res.* **478,** 337–348.
43. McAllister J. P. and Das G. D. (1977) Neurogenesis in the epithalamus, dorsal thalamus and ventral thalamus of the rat: An autoradiographic and cytological study. *J. comp. Neurol.* **172,** 647–686.
44. Mihailoff G. A., Kosinski R. J., Aziz S. A. and Border B. G. (1989) Survey of noncortical afferent projections to the basilar pontine nuclei: a retrograde tracing study in the rat. *J. comp. Neurol.* **282,** 617–643.
45. Mok D. and Mogenson G. J. (1986) Contribution of zona incerta to osmotically induced drinking in rats. *Am. J. Physiol.* **251,** R823–832.
46. Mok D. and Mogenson G. J. (1987) Convergence of signals in the zona incerta of angiotensin-mediated and osmotic thirst. *Brain Res.* **407,** 332–340.
47. Nicolelis M. A. L., Chapin J. K. and Lin R. C. S. (1991) Ontogeny of corticocortical projections of the rat somatosensory cortex. *Somat. Motor Res.* **8,** 193–200.
48. Nicolelis M. A. L., Chapin J. K. and Lin R. C. S. (1992) Somatotopic maps within the zona incerta relay parallel GABAergic somatosensory pathways to the neocortex, superior colliculus, and brainstem. *Brain Res.* **577,** 134–141.
49. Nicolelis M. A. L., Chapin J. K. and Lin R. C. S. (1991) Neonatal whisker removal in rats stabilizes a transient projection from the auditory thalamus to the primary somatosensory cortex. *Brain Res.* **567,** 133–139.
50. Ortel W. H., Tappaz M. L., Berod A. and Mugnaini E. (1982) Two-color immunohistochemistry for dopamine and GABA neurons in rat substantia nigra and zona incerta. *Brain Res. Bull.* 9, 463–474.
51. Porter L. L. and White E. L. (1983) Afferent and efferent pathways of the vibrissal region of primary motor cortex in the mouse. *J. comp. Neurol.* **214,** 279–289.
52. Ricardo J. A. (1981) Efferent connections of the subthalamic region in the rat. II. The zona incerta. *Brain Res.* **214,** 43–60.
53. Rieck R. W., Huerta M. F., Harting J. K. and Weber J. T. (1986) Hypothalamic and ventral thalamic projections to the superior colliculus in the cat. *J. comp. Neurol.* **243,** 249–265.
54. Roger M. and Cadusseau J. (1985) Afferents to the zona incerta in the rat: a combined retrograde and anterograde study. *J. comp. Neurol.* **241,** 480 492.
55. Romanowski C. A. J., Mitchell I. J. and Crossman A. R. (1985) The organization of the efferent projections of the zona incerta. *J. Anat.* **143,** 75–95.
56. Rose J. E. (1942) The ontogenetic development of the rabbit's diencephalon. *J. comp. Neurol.* **77,** 61–129.
57. Saper C. B. (1985) Organization of the cerebral cortical afferent systems in the rat. II. Hypothalamocortical projections. *J. comp. Neurol.* **237,** 21–46.
58. Saper C. B., Akil H. and Watson S. J. (1986) Lateral hypothalamic innervation of the cerebral cortex: Immunoreactive staining for a peptide resembling but immunochemically distinct from pituitary/arcuate α-melanocyte stimulating hormone. *Brain Res. Bull.* **16,** 107–120.
59. Sato K., Zhang J. H., Saika T., Sato M., Tadas K. and M. Tohyama (1991) Localization of glycine receptor α1 subunit mRNA-containing neurons in the rat brain: an analysis using *in situ* hybridization histochemistry. *Neuroscience* **43,** 381–395.

60. Sawyer S. F., Martone M. E. and Groves P. M. (1991) A GABA immunocytochemical study of rat motor thalamus: light and electron microscopic observations. *Neuroscience* **42,** 103–124.
61. Schlumpf M., Schoemaker W. J. and Bloom F. E. (1980) Innervation of embryonic rat cerebral cortex by catecholamine-containing fibres. *J. comp. Neurol.* **192,** 361–376.
62. Sequier J. M., Richards J. G., Malherbe P., Price G. M., Mathews S. and H. Möhler (1988) Mapping of brain areas containing RNA homologous to cDNAs encoding the α and β subunits of the rat $GABA_A$ γ-aminobutyrate receptor. *Proc. natn. Acad. Sci. U.S.A.* **85,** 7815–7819.
63. Senft S. L. and Woolsey T. (1987) Development of afferents to mouse somatosensory cortex. *Proc. Soc. Neurosci.* **13,** 1115 (Abstr.).
64. Senft S. L. (1990) Prenatal central vibrisssal pathway labeled with Dil and DiA. *Proc. Soc. Neurosci.* **16,** 1215 (Abstr.).
65. Shammah-Lagnado S. J., Negrao N. and Ricardo J. A. (1985) Afferent connections of the zona incerta: a horseradish peroxidase study in the rat. *Neuroscience* **15,** 109–134.
66. Shiosaka S., Shibasaki T. and Tohyama M. (1984) Bilateral α-melanocyte stimulating hormonergic fiber system from zona incerta to cerebral cortex:combined retrograde axonal transport and immunohistochemical study. *Brain Res.* **309,** 350–353.
67. Smith R. L. (1973) The ascending fiber projections from the principal sensory trigeminal nucleus in the rat. *J. comp. Neurol.* **148,** 423–446.
68. Starzl T. E., Taylor C. W. and Magoun H. W. (1951) Ascending conduction in reticular activating system, with special reference to the diencephalon. *J. Neurophysiol.* **14,** 461–477.
69. Steriade M., Parent A., Ropert N. and Kitsikis A. (1982) Zona incerta and lateral hypothalamic afferents to the midbrain reticular core of cat: an HRP and electrophysiological study. *Brain Res.* **238,** 13–28.
70. Taylor A. M., Jeffery G. and Lieberman A. R. (1986) Subcortical afferent and efferent connections of the superior colliculus in the rat and comparisons between albino and pigmented strains. *Expl Brain Res.* **62,** 131–142.
71. Villalobos J., Beracochea D. and Jaffard R. (1990) Age-related changes in the subcortical afferents to the medial frontal cortex in mice: a WGA-HRP study. *Neurosci. Lett.* **119,** 97–100.
72. Vincent S. R., Hokfelt T., Skirboll L. R. and Wu J. Y. (1983) Hypothalamic γ-aminobutyric acid neurons project to the neocortex. *Science* **220,** 1309–1311.
73. Watanabe K. and Kawana E. (1982) The cells of origin of the incertifugal projections to the tectum, thalamus, tegmentum and spinal cord in the rat: a study using the autoradiographic and horseradish peroxidase method. *Neuroscience* **7,** 2389–2406.
74. Wise S. P. and Jones E. J. (1978) Developmental studies of thalamocortical and commissural connections in the rat somatic sensory cortex. *J. comp. Neurol.* **178,** 187–208.
75. Wong-Riley M. T. T. and Welt C. (1980) Histochemical changes in cytochrome oxidase of cortical barrels after whisker removal in neonatal and adult mice. *Proc. natn. Acad. Sci. U.S.A.* **77,** 2333–2337.
76. Wong-Riley M. T. T. (1989) Cytochrome oxidase: an endogenous metabolic marker for neuronal activity. *Trends Neurosci.* **12,** 94–101.
77. Woolsey T. A. and Van der Loos H. (1970) The structural organization of layer IV in the somatosensory region (SI) of the mouse cerebral cortex: the description of a cortical field composed of discrete cytoarchitectonic units. *Brain Res.* **17,** 205–242.
78. Yamamoto T., Ochalski A., Hertzberg E. L. and Nagy J. I. (1990) LM and EM immunolocalization of the gap junctional protein connexin43 in rat brain. *Brain Res.* **508,** 751–760.
79. Yamamoto T., Ochalski A., Hertzberg E. L. and Nagy J. I. (1990) On the organization of astrocytic gap junctions in rat brains as suggested by LM and EM immunohistochemistry of connexin43 expression. *J. comp. Neurol.* **302,** 853–883.
80. Yamamoto T., Vukelic J., Hertzberg E. L. and Nagy J. I. (1992) Differential anatomical and cellular patterns of connexin43 expression during postnatal development of rat brain. *Devl Brain Res.* **66,** 165–180.
81. Yasui Y. Y., Itoh K., Kamiya H., Ino T. and Mizuno N. (1988) Cingulate gyrus of the cat receives projection fibers from the thalamic region ventral to the ventral border of the ventrobasal complex. *J. comp. Neurol.* **274,** 91–100.
82. Zamir N., Skofitsch G. and Jacobowitz D.M. (1986) Distribution of immunoreactive melanin-concentrating hormone in the central nervous system of the rat. *Brain Res.* **373,** 240–245.

(*Accepted* 9 *September* 1994)